

1 **DIATOM AND VEGETATION RESPONSES TO LATE GLACIAL AND EARLY-HOLOCENE**
2 **CLIMATE CHANGES AT LAKE ESTANYA (SOUTHERN PYRENEES, NE SPAIN).**

3

4 ¹Vegas-Vilarrúbia T., ² González-Sampéris P., ³Morellón M., ² Gil-Romera G., ² Pérez-Sanz A; ²Valero-
5 Garcés B.

6 ¹ Dep. Ecology, Fac. Biology, University of Barcelona, Barcelona, Spain. Email: tvegas@ub.edu. Phone:
7 +34 93 4031376

8 ² Pyrenean Institute of Ecology, Spanish Scientific Research Council, (CSIC), Zaragoza, Spain.

9 ³ Instituto de Geociencias, CSIC,UCM. Facultad de Ciencias Geológicas, Univ. Complutense. Madrid,
10 Spain.

11

12 **ABSTRACT**

13 We investigate Lake Estanya's diatom and pollen records from the Late Glacial (LG) to the Early Holocene
14 (EH), in order to compare limnological and vegetation responses to common climate forcing. The biotic
15 changes recognized in this study largely agree with the hydrological evolution of the lake described
16 previously for the same period. The diatom record shows high sensitivity to fluctuations in both lake level
17 and salinity concentration as consequence of climate shifts. In addition vegetation results indicate that the
18 area could have played an important role as regional vegetation refuge. Shallow lake conditions during the
19 Last Glacial Maximum (LGM) were punctuated by relatively deeper freshwaters between 19.3 and 18.6 cal
20 kyr BP and at 18.0 cal kyr BP, as recorded by diatom shifts. A subsequent increasing aridity trend,
21 coinciding with the Mystery Interval (MI), affected the diatom accumulation rates, which dropped to its
22 minimum values between 17.2 to 14.7 cal kyr BP. Particularly dry and cold conditions during the LGM and
23 MI are supported by the largest values of steppic pollen taxa of the whole sequence, which account for up to
24 40%. However, relatively high values of *Betula* during the Heinrich Event 1 suggest a plausible regional
25 vegetation refuge. Abrupt cooling and warming episodes within the LG triggered remarkable ecological
26 threshold crossings in the diatom communities, especially during the stadial/interstadial episodes. At this
27 point, the vegetation reflect the onset of warm conditions during the Bølling/Allerød with the partial
28 substitution of *Betula* by Marcescent and Evergreen *Quercus*, what probably indicates the arrival of

29 temperate taxa to the area and the likely migration of birch to higher altitudes. The Younger Dryas Stadial
30 shows a complex ecological response. Diatoms are very poorly preserved, but aquatic taxa reach their
31 highest values. An increase in Marcescent *Quercus* during this cold stage lends further support to the
32 hypothesis that this is a regional vegetation refuge. Low lake levels recorded during the EH affected the
33 development and preservation of diatom communities. A delay in the onset of humid conditions for the EH
34 is also supported by the vegetation composition, characterized by the maximum expansion of *Juniperus*.

35

36 **Keywords:** Biological responses, Diatoms, Ecological threshold, Mediterranean basin, Multiproxy
37 approach, Paleoecology, Paleolimnology.

38

39

40

41

42

43

44

45

46

47

48

49

50

51

52

53

54

55

56

57 **1. INTRODUCTION**

58 Forecasting the nature and magnitude of future biotic responses to climate change requires understanding of
59 the complexity of system response to climate forcing at different temporal scales (IPCC 2007). Although it
60 is often argued that the climate change predicted for this century is unprecedented due to its high rate of
61 change and magnitude, some of the climate oscillations during the last glacial cycle (ca. 120.0-11.6 kyr BP)
62 in the northern Hemisphere were also “abrupt” and “rapid”, typically occurring at a centennial or decadal
63 scale (Broecker 2000). For example, the North Atlantic Dansgaard/Oeschger cycles (Dansgaard et al. 1993;
64 Grootes et al. 1993) and the Heinrich events (Bond et al. 1992; Broecker 1994) alternated gradual cooling
65 with abrupt warming. Particularly, the rapid warming trend at the end of the Younger Dryas and the
66 beginning of the Holocene (Dansgaard et al. 1989) has been proposed as a possible past climate analogue,
67 because both magnitude and rates of change parallel those predicted for the present century (Jackson and
68 Overpeck 2000; Steffensen et al. 2008; Vegas-Vilarrúbia et al. 2011)

69 The available Iberian records show rapid hydrological, environmental and climate changes during the last
70 glacial cycle and suggest a strong link between the Western Mediterranean and the North Atlantic climate
71 (Pérez-Obiol and Julià 1994; Valero-Garcés et al. 1998; Cacho et al. 1999, 2001; González-Sampériz et al.,
72 2006; Moreno et al. 2010, 2012). A conspicuous regional feature for the last 25,000 years is that most of the
73 North Atlantic cooling events correspond to drought periods, as deduced from dust accumulation (Moreno
74 et al. 2002), speleothem records (Moreno et al. 2009), lacustrine sequences (Moreno et al. 2012) and both
75 marine (Fletcher and Sánchez-Goñi 2008) and continental pollen sequences (González-Sampériz et al.
76 2010; Carrión et al. 2010).

77 Biotic responses to climate change during the Late Glacial and Early Holocene in most western
78 Mediterranean regions have been mostly assessed using palynological records while other key
79 palaeolimnological variables like diatoms, ostracods or chironomids, which offer independent responses to
80 palaeoclimatic variables, have been comparatively less well studied. Pollen records show that vegetation
81 responses during periods of rapid climate change, particularly at a local scale, also depend on
82 autoecological processes, the proximity to refuge areas and/or high regional topographical variability
83 (Carrión et al. 2010). Lacustrine diatoms are very sensitive to changes in water balance and conductivity
84 and consequently have a great potential to test hypotheses of climate fluctuations, especially in regions with

85 a marked alternation between dry and wet phases like closed basins in the Mediterranean region (Ryves et
86 al 1996; Reed et al. 2010). Diatoms have short life cycles and show a rapid, species-specific responses to
87 variations in the precipitation/evaporation ratio (P/E) that in turn affect important limnological variables,
88 i.e. water temperature, lake level, salinity and nutrients concentration and lake productivity (Battarbee et al.
89 2001; Adrian et al. 2009). For instance, diatoms provided a clear evidence for the Younger Dryas reversal
90 to cold and arid conditions in Ioannina sequence, northwest Greece, where vegetation response was
91 apparently inhibited (Lawson et al. 2004; Wilson et al. 2008). In the Iberian Peninsula, diatom records are
92 really scarce, particularly for the Late Glacial and Early Holocene. However, the existing sequences show,
93 for example, a clear response to Early Holocene climatic shift in lakes from NW – Lake Lucenza (Leira and
94 Santos 2002) and Lagoa Grande (Leira 2005)- and SW Iberia - Laguna Medina- (Reed et al., 2001), and
95 more subdued changes in mountain areas (Lake Enol, Moreno et al. 2009). These records show a complex
96 hydrological variability and associated response in the Iberian Peninsula.

97 Our approach to better understand the nature, speed and thresholds of biological responses to gradual and
98 rapid past climate shifts is based on a multidisciplinary strategy applied to lacustrine sequences, including
99 pollen, diatom, sedimentological and geochemical techniques to assess the terrestrial vegetation, lake biota
100 and paleohydrological history, and the leads and lags of the different sub-systems to particular climatic
101 events.

102 Lake Estanya sequence (Morellón et al. 2009a, b) provides an opportunity to illustrate this approach
103 because the main hydrological and environmental changes during the last 20 kyr have been documented
104 using several proxies (sedimentary facies, elemental and isotopic geochemistry and biogenic silica) and a
105 robust age model. In this paper we investigate the nature of ecological responses of diatom communities
106 and vegetation to climate changes recorded between ca. 20-9.5 kyr BP in Lake Estanya, and we evaluate the
107 local and regional factors modulating the respective biotic responses.

108

109 **2. REGIONAL SETTING**

110 Balsas de Estanya (42°02' N, 0°32' E) is a karstic lake complex in a small (2.45 km²) endorheic basin
111 located at the southern foothills of the External Pyrenean Ranges in north-eastern Spain (Fig.1). These
112 mountain ranges are mainly composed of Mesozoic formations, and large poljes and dolines occur as the

113 result of karstic processes affecting Upper Triassic carbonate and evaporite materials outcropping along
114 geological structures (IGME 1982). The Balsas de Estanya consists of three dolines, two of them with water
115 depths of about 7 m and 20 m and one seasonally flooded (Fig. 1b). The region has a Mediterranean
116 continental climate with long summer droughts (León-Llamazares 1991). Mean annual temperature (MAT)
117 is 14 °C (from MAT of 4 °C in January to 24°C in July); mean annual precipitation (MAP) is 470 mm (from
118 MAP of 18 mm in July to 50 mm in October). The Estanya lakes are located at 670 m a. s. l. at the
119 boundary between the *Quercus rotundifolia* and the *Quercus faginea* forest communities corresponding to
120 the transitional zone between the Mediterranean and Sub-Mediterranean bioclimatic regimes (Blanco-
121 Castro et al. 1997) (Fig.1a). Nowadays, the lakes are embedded in a patchy landscape of natural vegetation
122 alternating with cereal crops. Hygrophyte communities of *Phragmites australis*, *Typha angustifolia*, *Juncus*
123 spp., and *Scirpus* spp. constitute the littoral belt (Avila et al. 1984; Cambra 1991).

124 This study focuses on the largest lake sub-basin, the “Estanque Grande de Abajo” (Lake Estanya), where
125 several cores have been recovered and studied (Morellón et al. 2009a, b). It has a relatively small watershed
126 (surface area of 106.5 Ha) and although there is no permanent inlet, several ephemeral creeks drain the
127 catchment, providing clastic material and run-off to the lake (López-Vicente 2007). The modern
128 hydrological balance of Lake Estanya is mainly controlled by evaporation output and groundwater inputs
129 (Morellón et al 2009a; Pérez-Bielsa et al. 2012). Maximum depth is about 20 m and slopes are steep, as
130 shown by the bathymetry (Figure 1). The basin is composed of two sinkholes separated by a shallower sill
131 (3 m max. depth) that emerges during low lake level periods. Measured electric conductivities (EC) are 630
132 $\mu\text{S}/\text{cm}$ in groundwater and 372 $\mu\text{S}/\text{cm}$ in surface water (Morellón et al., 2009a). Waters are alkaline and
133 sulphate and calcium rich, with a long residence time and a strong impact of evaporation upon the lacustrine
134 system. The thermal regime is monomictic with thermal stratification and bottom anoxia from May to
135 October. Concentrations of nitrogen and phosphorus are very low but experience a fast turnover, as
136 suggested from the fairly high phytoplankton concentrations ($> 10,000$ cells/ml). The summer maximum of
137 phytoplankton is dominated by *Planctonema lauterbornii* and other Chlorophyceae, while the cyanophyte
138 *Anabaena inaequalis* appears when nitrates are almost exhausted. At the end of summer Dinophyceae take
139 over with *Peridinium volzii*. Centric diatoms *Cyclotella comta* and *Cyclotella comensis* proliferate in
140 November during mixing of the water column and persist till spring, but disappear during summer (Ávila et

141 al. 1984).

142

143 **3. MATERIALS AND METHODS**

144 **3.2. Diatom analysis**

145 The composite sequence based on cores 1A and 5A from the deep sub-basin (Morellón et al., 2009a) was
146 sampled for diatom and pollen analyses. Fifty nine samples for diatom analysis were collected at 10-cm
147 intervals along the late glacial-Early Holocene interval. Diatoms were extracted from 0.1 g of dry sediment
148 and oxidised with hydrogen peroxide. Specimens were mounted in Naphrax and analyzed with a Polyvar
149 light microscope at 1000X magnification. Valve concentrations per unit weight of sediment were calculated
150 using plastic microspheres (Battarbee 1986) and transformed to diatom accumulation rates ($\text{valves} \cdot \text{cm}^{-1} \cdot$
151 yr^{-1}). At least 300-500 valves were counted in each sample whenever possible; when diatom content was
152 very low, counting continued until reaching at least 1,000 microspheres. Species were expressed in terms of
153 relative abundance (%) of each taxon (Flower 1993; Battarbee et al. 2001; Abrantes et al. 2005). Taxonomic
154 identifications and a review of autecological requirements for the principal taxa were made using
155 specialized literature (Krammer and Lange-Bertalot 1986, 1988, 1991, 2001; Van Dam 1994; Witkowski et
156 al. 2000; Lange-Bertalot 2001 a,b; Krammer 2002; Hofmann et al. 2011). We used the centric to pennate
157 diatom ratio (C/P) as an indicator of the relative abundance of planktonic to benthic habitat availability as a
158 proxy for lake level, although it is also known to indicate trophic changes mainly in disturbed environments
159 (Cooper 1995). The dissolution index, or the degree of diatom preservation expressed by the ratio of valves
160 showing dissolution and/or breakage to total valves number, yielded a mean value of 70%. Both phenomena
161 indicate the impact of diagenesis as well as the importance of silicification for diatom preservation (Flower
162 1993; Ryves et al. 2001). Sometimes differential preservation among species might not properly reflect the
163 diagenetic properties of the sediment (Reed et al. 2010). In our case, the central areas of most *Cyclotella*
164 taxa remained relatively well preserved, so they were easily identified and hence did not interfere with
165 counting accuracy. Fragilariales were commonly well preserved, while other taxa show variable
166 preservation, yet the most representative taxa could be identified reliably. Diatom diagrams were plotted
167 with Psimpoll software and divided into biozones using the Optimal Splitting by Information Content
168 Method (Bennett 1996). Only taxa showing abundances $> 3\%$ were illustrated.

169 Canonical Correspondence Analysis (CCA) was applied to elucidate the relationships between biological
170 assemblages of species and their environment. We previously run a Detrended Correspondence Analysis on
171 the species matrix and obtained a gradient length (range of the site scores) of 6.6 standard deviations,
172 which is an approximate measure of the existent ecological gradient in species turnover units and supports
173 an unimodal distribution of species abundance (Legendre and Legendre 1998). CCA was performed on
174 species abundance (explained variables) and XRF data counts of S, Ca, Al, K, Si, Fe, Ti from Morellón et
175 al. (2009b) (constrained, explanatory variables). Although element chemical concentrations in sediments
176 do not directly reflect water chemical composition, both are strongly related. Sediment composition is
177 strongly influenced by the same drivers controlling diatom variability i.e. changes in the trophic status,
178 salinity, lake-level fluctuations, clastic inputs. We used the Paleontological Statistics Software Package
179 PAST (Hammer et al. 2001); samples without quantifiable valve quantities were ignored. In CCA triplots,
180 the length of the arrows representing environmental variables is proportional to their rate of change, small
181 angles imply high positive correlations between variables, and arrows pointing in opposite directions will be
182 negatively correlated. Species are represented by their niche centre along each axis, i.e. by the weighted
183 average of the axis-scores of sites in which they occur. Thus, orthogonal projection of species along the
184 arrow permits comparisons of the relative effects of a particular variable on a diatom species. Orthogonal
185 projections close to an arrow tip indicate a strong effect of the variable on the pattern of variation of a
186 species. Eigenvalues sum (trace) is tested for significance using the method of permutations to determine
187 whether there is an overall relationship between species and environment (Legendre and Legendre 1998).

188

189 **3.3. Palynological analysis**

190 Palynological samples were extracted every 10-cm intervals, intercalated about 5 cm from diatom samples.
191 Pollen analyses followed the classic chemical method (Moore et al. 1991) modified according to Dupré
192 (1992), thus, including HCl, KOH, HF digestion and mineral-organic particles separation with Thoulet
193 solution (2.0 gr/cm³ density). *Lycopodium clavatum* tablets were added in order to calculate pollen
194 concentrations (Stockmarr 1971) and a minimum of 250-300 terrestrial pollen grains were counted in all
195 samples. Some samples (e.g. 850 and 600 cm depth) had very low pollen preservation and only 150-200
196 pollen grains could be counted. Palynological identification was completed under an optical microscope

197 (x400, x630 and x1000 magnification) using European pollen type keys (Moore and Webb 1978) and the
198 IPE-CSIC (Zaragoza, Spain) pollen reference collection. A total taxonomic diversity of 114 taxa was found
199 but only some groups and significant curves for interpretation were included in the pollen diagram, plotted
200 using Psimpoll 4.27 and divided into biozones using the Optimal Splitting by Information Content Method
201 (Bennett 2009).

202

203 **4. RESULTS**

204 **4.1. Chronology**

205 The chronology for the lake sequence was constrained by 21 accelerator mass spectrometry (AMS)
206 radiocarbon dates (Morellón et al., 2009a, b). In this paper we have re-calibrated the original radiocarbon
207 dates with the INTCAL09 curve (Reimer et al. 2011) using CALIB 6.0 software and improve the
208 correlation between cores 1A and 5A. The reservoir effect correction was applied following the approach
209 used in Morellón et al., (2009a,b) and consistently, age/depth relationship was obtained with a generalized
210 mixed-effect regression (Heegaard et al. 2005). Based on this revised age-depth model for Lake Estanya
211 record the ca. 10 m of sediment sequence spans from ca 19.5 k cal yrs BP to the present, and the average
212 error confidence interval is ca 150 kyr (Fig. 2 A). The sequence analysed in this paper spans the Late
213 Glacial to Early Holocene (ca. 19,5 to 9,5 cal kyr BP) (Fig. 2B). Linear sedimentation rates are four times
214 higher for clastic-dominant intervals (1.6 mm/yr) than for fine-laminated intervals (0.4 mm/yr) (Fig.2). The
215 detailed, chronological model and sedimentary and geochemical characteristics of the composite
216 sedimentary record of L. Estanya are described in Morellón et al. (2009a,b).

217

218 **4.2. Diatom analysis**

219 **4.2.1. Stratigraphy**

220 Figure 3 displays diatom accumulation rates and summarizes relative species abundance and the five major
221 diatom assemblage zones (DZ-EST 1 to DZ-EST 5) defined statistically. Diatom zone DZ-EST 2 includes a
222 number of main shifts within the diatom record and is further subdivided into eleven subzones (Fig. 3b;
223 subzones a- k).

224

225 *DZ-EST 1 (970-950 cm; ca.19, 665– 19,463 cal yr BP)*

226 In this zone, only pennate diatoms are present and in scant quantities ($3.53 \cdot 10^4$ to $2.39 \cdot 10^5$ valves \cdot cm⁻¹ \cdot
227 yr⁻¹) (2 samples). Assemblages are dominated by the epipelagic *Diploneis ovalis* (Hilse in Rabenhorst) Cleve
228 189 and the epiphytic *Epithemia adnata* (Kützing) Rabenhorst (1853). Other rarer taxa include *Mastogloia*
229 *smithii* Thwaites in W. Smith (1856) and *Navicula subalpina* Reichard. C: P ratio is always < 1. These
230 species have in common their preference for habitats with mid to high electrolyte content, mainly alkaline
231 waters in continental waterbodies.

232

233 *DZ-EST 2 (950- 660 cm; ca. 19,463 – 13,477 cal yr BP)*

234 In this zone the diatom accumulation rates increase markedly, from zero to $4.35 \cdot 10^7$ valves \cdot cm⁻¹ \cdot yr⁻¹,
235 reaching high but very fluctuating values (29 samples). C: P ratio is always >1. The zone is characterized by
236 rapid changes in diatom community, mostly dominated by the centric diatom *Cyclotella ocellata* Pantocsek
237 (valves with 3 ocelli), which largely determines the trends in the diatom accumulation rates. At the
238 transition between zones DZ-EST 1 and DZ-EST 2 (subzone k) *Cyclotella ocellata* replaces *Diploneis*
239 *ovalis* and shows a first peak at 945 cm, followed by a strong decrease. The interval between 936 and 920
240 cm is barren of diatoms except for some traces of *Campylodiscus* Ehrenberg ex Kützing (1844) sp.
241 fragments but soon thereafter, *C. ocellata* expands again and dominates until 860 cm (subzone j). The
242 marked decline in subzone I coincides with the reappearance of *Diploneis ovalis* and the occurrence of
243 other pennate taxa such as the epiphytic *Cocconeis placentula* Ehrenberg, the cosmopolitan *Encyonopsis*
244 *subminuta* Krammer & E. Reichardt and *Encyonema caespitosum* Kützing, *Mastogloia smithii* and
245 *Navicula* Bory sp. 9, although these latter species appear in very low percentages. They coexist with low
246 abundances of *Cyclotella ocellata*, until this latter species expands again (subzone h) at the expense of
247 pennate taxa and becomes dominant again between 810 -750 cm (subzone g). During subzone g another
248 centric diatom, *C. distinguenda* Hustedt, a pelagic inhabitant of alkaline waters, coexists with *C. ocellata*,
249 although in relatively low proportions. *C. distinguenda* becomes dominant in 760-750 cm (subzone f), but
250 *C. ocellata* soon recovers hegemony (subzone e). After a short interval with only traces of diatoms (750 and
251 740 cm depth, subzone d), *C. ocellata* populations reappear and show two maxima at 710 (subzone c) and at
252 680 cm (subzone a) reaching the highest value of the whole zone DZ-EST 2. The strong decrease in

253 subzone b coincides with a slight increase of some pennate species such as *Amphora inariensis* Krammer,
254 *Sellaphora pupula* (Kützing) Mereschkowsky, *Cocconeis placentula*, and some species of the genus
255 *Mastogloia* Thwaites. The transition zone to DZ-EST3 (subzone a) is abrupt and characterized with the
256 proliferation of small quantities of *Amphora veneta* var. *subcapitata* Kisselew, *Nitzschia* cf. *filiformis* (W.
257 Sm.) Van Heurck, *Fallacia pygmaea* (Kützing) A.J.Stickle & D.G.Mann, *Tryblionella hungarica* (Grunow)
258 D.G.Mann, *Denticula elegans* Kützing and some species of the genera *Navicula*, *Pinnularia* Ehrenberg and
259 *Mastogloia*.

260

261 *DZ-EST 3 (660- 610 cm; ca. 13,477-12,502 cal yr BP)*

262 This zone is characterized by scarce diatom presence and valve accumulation rates ranging from zero to
263 $8.77 \cdot 10^4$ valves \cdot cm⁻¹ \cdot yr⁻¹ (6 samples). Where diatoms occur, C: P ratio is always < 1. The species
264 assemblage characterizing the transition between zones DZ-EST2 and DZ-EST3 is replaced by an
265 assemblage of pennate diatoms typical of aerophytic and subaerial habitats such as *Hantzschia amphioxus*
266 and *Luticola mutica*. Also *Navicula salinarum* (Grunow 1880), known from marine and inland tidal
267 habitats, it is very common in ephemeral Spanish salt lakes (Reed 1998) and appears for the first time in the
268 record;

269

270 *DZ-EST 4 (610- 460 cm, ca. 12,502 – 9,543 cal yr BP)*

271 Most of the zone is devoid of diatoms. At the onset of this zone there are small peaks of freshwater diatoms
272 as *Cyclotella ocellata* and *Cyclotella distinguenda*, and larger peaks of *Mastogloia smithii*, common in
273 fresh- and brackish waters, and *Mastogloia braunii* Grunow, common in brackish-waters of saline inland
274 waters. C: P ratio keeps < 1. There are some diatom traces at 562.5 cm depth and an isolated diatom peak at
275 503 cm ($2.95 \cdot 10^5$ valves \cdot cm⁻¹ \cdot yr⁻¹), nearly exclusively composed by the cosmopolite species
276 *Pseudostaurosira brevistriata* (Grunow) D.M.Williams & Round, characteristic of fresh- or, oligosaline and
277 calcium-rich waters.

278

279 *DZ-EST 5 (460 – 416.5 cm, ca. 9,543 – 9,375 cal yr BP)*

280 The beginning of the zone is marked by the return of *Pseudostaurosira brevistriata* as dominant species and
281 the presence of *C. ocellata*. Valve accumulation rates ranges between $2.37 \cdot 10^3$ and 1.12×10^5 valves $\cdot \text{cm}^{-1} \cdot$
282 yr^{-1} . *Pseudostaurosira brevistriata* shows a minimum at the upper part of the core, with minor increases of
283 *Luticola mutica* (Kützing) D.G.Mann and *Hantzschia amphioxys* (Ehrenberg) Grunow and smaller peaks of
284 *Epithemia adnata*, *Denticula elegans*, *Amphora* spp. and *Mastogloia* spp. Towards the top of the zone
285 *Pseudostaurosira brevistriata* increases again at the expenses of the other species.

286

287 **4.2.2. Canonical correspondence analysis**

288 The overall test of significance shows that canonical relationship between response (diatoms) and
289 explanatory variables (XRF data) is significant ($p = 0.03$, 1000 permutations). The eigenvalue of the first
290 eigenvector is $\lambda_1 > 0.3$ indicating a rather strong gradient (Table 1) (ter Braak and Verdonschot 1995). The
291 first eigenvectors account respectively for 34.7%, 25.4% and 18.2% of total variation in response variables.
292 Eigenvector 1 is positively correlated with Ca, S and negatively with Fe; eigenvector 2 shows weak and
293 inverse correlations with Ca and S, and eigenvector 3 has negative significant correlations with K, Fe and Ti
294 (Table 1). Si, K, Ti and Fe are strongly correlated with each other, reflecting their origin as clastic input
295 from the lake basin although Si may partially be biogenic silica. Ca is present in clastic carbonates and in
296 endogenic phases formed within the lake through inorganic or biological processes, whereas S may be
297 associated mainly with gypsum and sulphate deposition, but perhaps also with sulphide precipitation under
298 temporary anoxic conditions. In the first triplot (Fig. 4a) Ca, Fe and S show the highest rates of change.
299 Sites (depths) scores appear scattered along eigenvectors 1 and 2 and roughly 40% remain clumped at the
300 upper quadrant of the graph, these sites belong to subzone DZ-Est 2. The order of the species' orthogonal
301 projections onto main arrows and their prolongations indicate their relative response/sensitivity to shifts in
302 the particular environmental variables In our case, all species located on the right side of the graphs 4b and
303 4d seem to react distinctly to shifts in Ca and S, whereas species located on the left side of the graph seem
304 to be related with Fe and Ti shifts. Some of the species best related to changes in Ca are *Denticula elegans*,
305 *Amphora libyca* Ehrenberg, *Navicula* sp. 9, *Encyonopsis microcephala* (Grunow) Krammer) and
306 *Mastogloia smithii*, while those better related to S are *Cyclotella* spp. Some of the species best related to
307 variations in K, Ti, and Fe are *Pinnularia borealis* (Ehrenberg), *Luticola nivalis*, *Cocconeis placentula*,

308 *Diploneis ovalis* and *Navicula salinarum*, as well as some undetermined species of *Mastogloia* and
309 *Navicula* (4d).

310

311 **4.3. Pollen analysis**

312 Five pollen zones -PZ-EST 1 to PZ-EST 5- (Fig. 5) are described for the Late Glacial and the beginning of
313 the Holocene in the L. Estanya sequence.

314

315 *PZ-EST 1 (965-720 cm depth, 19,700-14,600 cal yr BP)*

316 Pollen preservation is low in this zone of the sequence, with sterile samples located at 890, 860, 825, 805,
317 785 and 728 cm depth (marked by grey bands in the pollen diagram, Fig. 5). The non-sterile samples show
318 similar palynological features: *Pinus* and *Juniperus* are the dominant taxa in the arboreal pollen group (AP),
319 with fluctuating proportions at around 20%, and herbaceous components Steppe taxa (Chenopodiaceae,
320 Caryophyllaceae, Urticaceae, *Rumex*, Cichorioideae, Asteroideae, Carduae, *Plantago*) and *Artemisia*
321 dominate and reach the highest values of the sequence (40%). The presence of *Betula* reaching 10%, the
322 occurrence of Marcescent *Quercus* in the upper part of this zone, the high values of *Ephedra dystachia* and
323 the almost complete absence of Mediterranean shrubs are characteristic of this zone. The aquatics show
324 very low percentages (< 5 %) and are dominated firstly by *Ranunculus* and then *Myriophyllum*.

325

326 *PZ-EST 2 (720-610 cm depth, 14,600-12,500 cal yr BP)*

327 This zone is characterized by a rapid development of forest taxa and a sharp decrease of *Artemisia* and
328 Steppe taxa (less than 10%). The forest is mostly composed by *Pinus* and *Juniperus* (values up to 60% and
329 30% respectively), with a relative increase of Marcescent *Quercus* and “Other mesophytes” and a decrease
330 in *Betula*. The hydro-hygrophytes group increases (mainly Cyperaceae, *Ranunculus* and *Potamogeton*). A
331 sterile level occurs at the top of this section (620 cm depth).

332

333 *PZ-EST 3 (610-570 cm depth, 12,500-11,600 cal yr BP)*

334 At the beginning of this zone, the AP composition drastically changes with a decrease of conifers (pines and
335 junipers, 10-20% and less than 10% respectively), while Marcescent *Quercus*, Evergreen *Quercus* and

336 Mediterranean shrubs develop. *Juniperus* slowly increases at the top of the zone. *Artemisia* and Steppe taxa
337 continue with low values, while the aquatics increase notably, with Cyperaceae, *Typha* and *Potamogeton*
338 showing the maximum percentages.

339

340 *PZ-EST 4 (570-500 cm depth, 11,600-9,900 cal yr BP)*

341 *Juniperus* spreads at the onset of this zone and becomes the dominant AP taxon (40 %) while all
342 mesophytes, both *Quercus* types and Mediterranean shrubs values are very low. Simultaneously, *Artemisia*
343 and Steppe taxa develop again while the proportions of aquatics decrease (both hygro- and hydrophytes).
344 *Ephedra dystachia* and *E. fragilis* types record their last relevant proportions in the sequence whereas
345 *Artemisia* and Steppe taxa values remain constant, somewhat decreasing, values. Aquatics present similar
346 proportions to the previous zone, without significant changes.

347

348 *PZ-EST 5 (500-400 cm depth, 9,900-8,900 cal yr BP)*

349 The onset of this zone is defined by a sharp increase in *Corylus* and the development of Marcescent
350 *Quercus*, “Other Mesophytes”, Mediterranean shrubs and Evergreen *Quercus*. *Juniperus* abruptly
351 decreases to less than 10% and pines recover to higher proportions (20-30%). Steppe taxa and *Artemisia*
352 diminish and an important hydro-hygrophites expansion (mainly Cyperaceae and *Potamogeton*) occurs.

353

354 **5. DISCUSSION**

355 Previous paleohydrological research carried out in the Lake Estanya sequence, based on sedimentology and
356 geochemistry (Morellón et al. 2009a), demonstrated a large hydrological variability during the last ca. 20
357 cal kyr BP, and particularly, within the Late Glacial period. The period 20 – 9.5 cal kyr BP was
358 characterized by arid conditions represented by shallow lake levels, predominantly saline waters and
359 reduced organic productivity. According to this reconstruction, the most arid conditions occurred during the
360 period 18 - 14.5 cal kyrs BP (including Heinrich event 1) and the Younger Dryas (12.9 – 11.6 cal kyrs BP).
361 Fresher conditions characterized the 14.5 - 12.6 cal kyrs BP period, likely indicating higher effective
362 moisture during the Bölling/Allerød. Finally, the onset of more humid conditions started at 9.4 cal kyrs,
363 indicating a delayed hydrological response to the beginning of the Holocene.

364 As the identified diatom and pollen zones broadly coincide, we have structured the discussion in five
365 periods of time in order to facilitate the comparison among them.

366

367 **5.1. The Last Glacial maximum (LGM) (19.7-18.0 cal kyr BP) and onset of Termination I**

368 The sedimentary and geochemical features indicate that Lake Estanya was relatively shallow, with a
369 fluctuating water balance and deposition of alternating carbonate and gypsum sediments (Morellón et al.,
370 2009). Several studies in lakes of the Iberian Peninsula and in marine records also suggest the occurrence of
371 periods of relative positive hydrological balance during the LGM in a context of the cold and dry climate
372 during LGM (see Cacho et al. 200, Moreno et al. 2012 and literature therein).

373 The diatom communities responded to these changes with alternating episodes of dominance of planktonic
374 *Cyclotella ocellata* and others with more development of benthic and littoral taxa. The base of the sequence
375 is dominated by the epipelagic diatom *Diploneis ovalis* that in the CCA analysis appears associated with
376 higher catchment erosion and runoff, and other benthic, alkaliphilous species like *Epithemia adnata*,
377 associated in the CCA triplots with periods of higher and fluctuating carbonate and sulphate deposition.
378 This assemblage is thus indicative of shallow, fluctuating conditions and alkaline waters. The substitution at
379 19.3 cal kyr BP of this assemblage by a planktonic community dominated by *Cyclotella ocellata* suggests
380 more permanent and deeper waters. *C. ocellata* is considered a cosmopolitan species that thrives in different
381 environments (Krammer and Lange-Bertalot 1986-2000), and in the European Diatom Database (EDDI) it
382 is most frequently reported in deep alkaline lakes. However, in Spain *C. ocellata* has also been found in
383 shallow lakes < 2m deep and is classified as a fresh- or oligosaline species, with a tolerance optimum of
384 0.81 mS/cm and with a tolerance range between 0.13 and 4.92 mS/cm (Reed 1998). At the end of this
385 period (18.6 cal kyr BP) the decrease of diatom accumulation rates ($1.73 \cdot 10^5$ valves/gr·yr) and the
386 occurrence of small proportions of most benthic and littoral taxa at the expenses of *C. ocellata* reflects an
387 expansion of littoral habitats or closer proximity to the littoral source area both likely related to lower lake
388 levels. At 18 cal kyr BP, a rapid increase in diatom accumulation rates points to a quick recovery of the
389 diatom community and a shift to a relatively deeper fresher lake, as inferred from the appearance of
390 *Cyclotella distinguenda*, an alkaliphilous diatom that has less tolerance to oligosaline conditions than *C.*
391 *ocellata* (Reed 1998) (estimated tolerance optimum of 0.62 mS/cm range between 0.33 and 1.16 mS/cm). In

392 the CCA analysis the abundance of this species appears slightly more sensitive to salinity variations than *C.*
393 *ocellata*.
394 Pollen data are also coherent with fluctuating hydrological conditions, well marked by Hygrophytes and
395 Hydrophytes changes and periods of even subaerial exposure with more intense oxidation processes leading
396 to numerous palynological sterile levels. *Artemisia* and Steppe taxa (Chenopodiaceae, Caryophyllaceae,
397 Urticaceae, *Rumex*, Cichorioideae, Asteroideae, Carduae, *Plantago*) reach more than 40% of the whole
398 pollen content while AP values fluctuates between 20-40%, dominated by pines, suggesting cold and
399 generally arid conditions. Other studies in lakes of the Iberian Peninsula and of marine records also suggest
400 the occurrence of periods of positive hydrological balance in a context of cold and dry climate during LGM
401 (see Moreno et al. 2012 and literature therein). According to our chronology, the decrease of diatom
402 accumulation rates and rapid changes in community composition in Lake Estanya are synchronous with the
403 alkenone SST decrease recorded in the Alboran sea about 18.7 to 18 cal kyr BP (Cacho et al. 2001).

404

405 **5.2. The Termination 1 and Mystery interval (18 – 14.5 cal kyr BP)**

406 The sedimentological record of L. Estanya (Morellón et al. 2009b) shows an aridification trend and the
407 gradual establishment of a closed, permanent lake with alkaline conditions (18.0 – 14.5 cal kyr BP).
408 Consistently, with a drier climate trend, diatom accumulation rates decreases after peaking at about 18.0 cal
409 kyrs BP and reaches minimum values between 17.2 to 14.7 cal kyr BP (Figs. 3 and 4).

410 The interval called “Mystery Interval”, including Heinrich event 1 (H1), is characterized as a global, cool
411 and arid period (Denton et al. 2006). The H1 onset (16.9 cal kyr BP) is clearly recorded in the sediment
412 record of L. Estanya by the substitution of finely laminated facies by clastic and banded gypsum facies
413 indicative of alternating flooding and desiccation with associated evaporative concentration, respectively
414 (Morellón et al 2009).

415 Other regional reconstructions also show colder and more arid conditions for this interval: the Alboran Sea
416 and Gulf of Cádiz (Cacho et al. 2001), El Portalet peatbog in the Pyrenees, (González-Sampéris et al.
417 2006), Lake Banyoles (Pérez-Obiol and Julià 1994; Valero – Garcés et al., 1998, Höbig et al., 2011) and
418 lake Siles (Carrión et al. 2002), for example. Our record does not show any diatom response to this
419 transition in terms of noticeable changes in community composition or accumulation rates (see clumped

420 samples and diatoms position in Fig. 6), where planktonic *Cyclotella* species remain dominant (Fig. 3,
421 subzones d,e,f of Fig. 4). This fact is probably due to low sampling resolution during this period.
422 As during the LGM, palynological spectra from the “Mystery Interval” (MI) in L. Estanya (790-720 cm
423 depth, Fig. 5) reflects a cool and arid climate, with a maximum expansion of Steppe taxa (especially
424 *Artemisia*), the maintenance of high abundance of conifers, which dominate the AP cover and low presence
425 or even absence of temperate taxa like Evergreen *Quercus* and Mediterranean shrubs. Values of *Pinus*
426 below 30% could reflect long-distance pollen transport or the existence of little patches of pine forest in the
427 proximity of the lake, while maximum values at around 10-20% (Huntley & Birks 1983) suggest that
428 *Juniperus* developed both regionally and locally. *Ephedra dystachia* type and *Artemisia* have their
429 maximum values of the whole sequence stressing the dominant arid conditions. The timing of *Artemisia*
430 peaks are in agreement with regional data that establish the maximum expansion of *Artemisia* in the
431 Pyrenees between 18-15 cal kyr BP (Jalut et al. 1992; Reille and Lowe 1993; González-Sampériz et al.
432 2006). The relatively high percentages of first *Betula* and then Marcescent *Quercus* at this time-interval in
433 L. Estanya are not consistent with the general arid climate conditions during the MI. We consider the
434 presence of these taxa as an indication of refuge areas for meso-thermophilous trees in the region. These
435 refuge locations were likely associated with sites with higher water availability along river valleys fed by
436 glacial melt water at the headwaters as it has been shown in other palaeoclimatic sequences of the Ebro
437 Basin and Iberia (Valero-Garcés et al. 2000, 2004; González-Sampériz et al. 2004, 2005, 2010; Carrión et
438 al. 2010).

439

440 **5.3. Abrupt cooling episodes within the Bölling / Allerød interstadial (14.5-12.8 cal kyr BP)**

441 The lack of accurate chronologies and high-resolution analyses in continental records has precluded the
442 identification of cold episodes within the Bölling / Allerød interstadial in the Iberian Peninsula. The Portalet
443 sequence in the central Pyrenees (González-Sampériz et al., 2006) provided the first evidence of abrupt and
444 rapid climate changes in terrestrial sequences during the deglaciation, synchronous to the North Atlantic
445 sequences. However, the timing and patterns of the abrupt climatic changes of the last deglaciation
446 identified in the paleorecords of the IP and how they reflect North Atlantic variability are still a matter of
447 debate (e.g.; Moreno et al. 2012). Sedimentological and geochemical data indicate that Estanya lake level

448 remained stable, with relatively shallow, saline conditions prevailing until 13.5 cal kyr BP, when lake
449 deposition returned to carbonate-rich facies up to 13.3 cal kyr BP indicative of a brief interval of brackish
450 water conditions and thus, a relatively more positive water balance in Lake Estanya (Morellón et al. 2009b).
451 Although the limited resolution hampers an accurate dating of the beginning or the end of these periods, our
452 data indicate a fast response of diatom communities of Lake Estanya to some of these rapid climatic
453 episodes. High diatom accumulation rates and dominance of *C. ocellata* observed between 14.5-13.5 cal kyr
454 BP suggest a positive hydrological balance throughout this period (see clumped samples and diatoms
455 position in Fig. 4), but punctuated by short episodes of decreasing diatom concentrations and associated
456 shifts in species assemblage composition (see position of samples 654 and 694, Fig. 4). For instance, a
457 decrease in diatom accumulation rates between 13.9 and 13.7 cal kyr BP is marked by the reappearance of
458 alkaliphilous diatoms inhabiting different littoral substrates at the expense of freshwater diatoms, pointing
459 to lake level instability and a partial return to shallower and brackish water conditions. Taking into account
460 dating uncertainties, this short episode leading to an ecological threshold cross broadly coincides with the
461 abrupt cooling of the Older Dryas reversal (14.1-13.9 cal kyr BP). The subsequent *C. ocellata* peak (13.6
462 cal kyr BP, one sample) could represent the first phase of the warm Allerød interstadial. Between 13.2 and
463 12.9 cal kyr BP (2 samples) *C. ocellata* disappears and the planktonic community is substituted by scant
464 populations of brackish/saline, subaerial and aerophytic diatom taxa, suggesting a second diatom ecological
465 threshold coinciding with shallower lake conditions, with some phases of subaerial exposure. Many species
466 dominating this assemblage are known from habitats with moisture variations and prone to drying out, i.e.
467 soils, sublittoral and damp sites and caves, mosses (Lange-Bertalot 2001 a,b; Poulíkova and Hasler 2007).
468 Additionally, from the presence firstly *Navicula salinarum* and secondly *Hantzschia amphioxys* with
469 estimated salinity optima of 8.9 and 39.0 mS/cm respectively (Reed 1998), we infer that environmental
470 conditions were probably brackish. This arid episode could correlate with the Intra Allerød Cooling Period
471 (13.2-12.9 cal kyr BP). A return of planktonic diatom community although in low abundances points to
472 slight recovery of lake level and could reflect the last phase of the Allerød Interstadial (12.9-12.7 cal kys
473 BP). The age model precluded a direct association of sedimentological and geochemical changes with the
474 known intra Bölling / Allerød interstadial variability (Morellón et al. 2009b). However, the diatom
475 fluctuations during this interstadial are consistent with the reconstructed paleohydrological and productivity

476 ($\delta^{13}\text{C}_{\text{org}}$) evolution evidencing a trend towards moister and warmer conditions with minor changes
477 promoted by short, abrupt climate changes, such as the Older Dryas (GI-1d) and the Inter Allerød Cold
478 Period (GI-1b) (Morellón et al. 2009b).
479 Pollen data from zone PZ-EST2 (Fig. 5) also identify the warming and increasing humidity trend during the
480 Bölling / Allerød interstadial, with a clear increase in the AP proportions that reach values of around 60-
481 80%. Despite the continued dominance of pines and junipers, at a local and regional scale (Jalut et al. 1992;
482 Montserrat 1992; González-Sampériz et al. 2005, 2006, 2008), relatively constant percentages of
483 Marcescent *Quercus* and Evergreen *Quercus* and the development of “Other Mesophytes” indicate warmer
484 temperatures. *Betula* proportions decrease notably suggesting the disappearance from the L. Estanya
485 surroundings and its migration to the highlands, in agreement with the global increase in temperatures
486 associated with this interstadial. A decreasing trend in Steppe taxa and the sharp drop of *Artemisia* also
487 point to moister conditions. The development of the aquatic component (mainly *Ranunculus*, Cyperaceae
488 and *Potamogeton*) would reflect a higher development of flooded environments in the basin area. The
489 current resolution does not enable the detection of vegetation responses to abrupt climate changes within the
490 B/A.

491

492 **5.4. The Younger Dryas stadial (YD) (12.7 -11.6 cal kyr BP)**

493 The YD stadial is characterized in L. Estanya by a lake-level drop and salinity increase as indicated by the
494 return towards the gypsum-rich facies and decrease in organic productivity (marked by positive excursion
495 of $\delta^{13}\text{C}_{\text{org}}$ and a sharp decrease in biogenic silica, compared to previous B/A values) (Morellón et al.
496 2009b). This salinity increase is reflected in the diatom record, by the appearance of *Mastogloia braunii*
497 which occurs for the first time in Estanya. From ~12.7 to 9.5 cal kyr BP diatoms are nearly or totally absent.
498 A likely explanation is that environmental conditions were inadequate for diatom colonization and/or
499 subsequent preservation, due to, for example: i) extremely alkaline conditions in concentrated waters
500 leading to frustules dissolution, perhaps exacerbated by an ephemeral lake state which tends to cause
501 increased breakage (Flowers 1993; Reed 1998), ii) eventual episodes of desiccation and competition with
502 macrophytes growth in an oligotrophic environment. Both hypotheses are supported by the sedimentary
503 record of L. Estanya indicating a lake level drop around 12.8 cal kyr BP (Morellón et al. 2009b) and by the

504 palynological record showing abundance of macrophytes pollen. The near absence of valves in this part of
505 the record prevents discerning diatom responses to the effects of cold and drought phases, characteristic of
506 this stadial. A similar situation is recorded in L. Enol (northwest IP) for the same period (Moreno et al
507 2009), as samples are barren of diatoms and the sedimentary record reflects a cold environment probably
508 depressing the lake's primary productivity.

509 The pollen spectra from L. Estanya sequence (PZ-EST3) do not have an unequivocal cold and arid signature
510 as expected during the Younger Dryas. However, lacustrine sequences from the IP show different responses
511 for the YD (Carrión et al. 2010). A drop in juniper's proportions and AP percentages as well as a new
512 increase in Steppe taxa is strong evidence for colder and more arid conditions but *Artemisia* percentages
513 remained similar. Besides, both Marcescent and Evergreen *Quercus*, and "Other Mesophytes" and
514 Mediterranean shrub proportions increase, suggesting a migration of these species towards the lowlands as a
515 result of lower temperatures at high altitude.

516 Finally, the aquatic taxa (macrophytes like *Potamogeton* and *Myriophyllum*) have their highest values of the
517 whole sequence suggesting that the lake never completely dried out in spite of regional aridity. This
518 increase in aquatic taxa during generally lower lake levels would rather reflect a higher development of
519 shallow water habitats. Thus, alkaline waters more than drying conditions seem to explain the poor diatom
520 preservation in L. Estanya during the YD interval. Considering that higher *Juniperus* values during the
521 Bölling/Allerød probably implied its local presence around Estanya basin, we propose that colder
522 temperatures during the YD caused an abrupt vegetation change with a reduction of this tree cover
523 reduction in an open landscape. In addition, these colder temperatures facilitated a migration of
524 mesothermophytes to lowlands, to refuge areas close to L. Estanya as occurred during Late Glacial times.

525 This situation could explain the unexpected proportions of Mesophytes and Mediterranean taxa recorded in
526 the L. Estanya pollen record during a cold and arid event like the YD. The abundance in the pollen record
527 of aquatic macrophytes including *Potamogeton* and *Myriophyllum* also corroborates that the lake did not
528 completely dry out in spite of regional aridity. This increase in aquatic taxa during generally lower lake
529 levels would reflect a higher development of shallow water habitats with higher light penetration in the
530 whole karstic complex, as a result of lower lake levels.

531

532 **5.5. Early Holocene (11.5 – 9.3 cal kyr BP)**

533 The sedimentary record shows that L. Estanya experienced a new water level drop after the YD, leading to
534 development of a shallow, ephemeral saline lake-mud flat complex with alternating carbonate
535 sedimentation during flooding and gypsum precipitation during desiccation phases (Morellón et al 2009b).
536 Adverse conditions for diatom colonization and/or preservation were maintained, as reflected by the
537 persistence of extremely low diatom accumulation rates and reduced diversity (Fig. 3).
538 Pollen data demonstrate that dry/arid conditions continued during the beginning of the Holocene (PZ-EST4,
539 11.5-9.9 cal kyr BP), with a maximum expansion of juniper, a clear decrease of Marcescent *Quercus*, Other
540 Mesophytes and *Corylus*, a new increase of *Ephedra dystachia* type and *Artemisia* values, and an abrupt
541 drop or even disappearance of both diversity and abundance of the aquatic taxa.
542 Scant amounts of diverse brackish diatom populations began to appear only after 9.5 kyr BP (5 samples), at
543 the same time as $\delta^{13}\text{C}$ shifts indicate enhanced algal productivity consistent with the onset of more humid
544 conditions (Morellón et al 2009b). Synchronously to these changes in diatom communities, *Corylus* and
545 Marcescent *Quercus* develop (PZ-EST5) while *Juniperus* drops abruptly reaching values under 10%
546 (compared to 50 % in previous zone PZ-EST4). Simultaneously both *Ephedra* types disappeared and the
547 aquatics recovered with the development of mainly Cyperaceae and *Potamogeton*, indicating some increase
548 in temperatures and general humid conditions.
549 A decoupling of the local hydrological response to global climate fluctuations is evidenced during this
550 period (Morellón et al. 2009a). Both diatom and pollen show a delayed local hydrological response at about
551 9.5 cal kyr BP compared to the increasing temperatures of the onset of the Holocene. Increased seasonality,
552 with higher summer insolation at mid-latitudes might have also amplified the hydrological response of Lake
553 Estanya, which is particularly sensitive to evaporation. Relatively dry conditions for the Early Holocene
554 have been recorded in other sequences of the Southern Pyrenees (e.g., Basa de la Mora: Pérez-Sanz et al., in
555 press). Continental sequences of the Iberian Peninsula based on different proxies (Pérez-Obiol and Julià
556 1994; Giralt et al. 1999; Carrión 2002; Leira 2005; Fletcher et al. 2007; Morellón et al 2009a, Moreno et al.
557 2009), indicate that hydrological and ecological response to the onset of the Holocene has a large regional
558 variability in the IP (see Carrión et al. 2010 and literature therein).

559

560 **5.6. Biotic responses to environmental and climatic changes along the L. Estanya record**

561 Diatom and vegetation communities show large and rapid changes during the Late Glacial to the Early
562 Holocene in Lake Estanya (Fig. 6), synchronous with the main paleohydrological and climate changes
563 reconstructed from sedimentological and geochemical data (Morellón et al., 2009a, b). Large environmental
564 fluctuations during the Late Glacial and Early Holocene are clearly recorded in the diatom assemblages
565 with periods of planktonic *C. ocellata* dominance alternating with periods of diverse non-planktonic
566 assemblages. From the CCA analysis we infer that changes in clastic input and/or carbonate and sulphate
567 deposition/redissolution coincide with significant changes in habitat conditions, since these processes
568 determine changes in limiting factors for diatom species, as for instance lake-level, salinity, mixing
569 dynamics and light penetration. For the same period Morellón et al. (2009 b) found clastic input, lake-level
570 and water salinity and the main factors forcing the sedimentary evolution of the sequence, mostly climate-
571 driven in a landscape with a relatively poor vegetation cover. These climate-driven environmental changes
572 may have triggered distinct diatom responses and even ecological thresholds leading to repeated
573 replacements of diatom assemblages along the record, especially during the Bölling / Allerød interstadial, in
574 less than 100-200 years (Fig. 6). The irreversibility of changes in diatom assemblages suggests the existence
575 of tipping points. The resulting assemblages are associated with the successive occurrence of very different
576 and contrasting habitat conditions within the lake. Catalan et al. (2009) showed diatom ecological threshold
577 to be associated with acid neutralizing capacity and ice-cover in European alpine-lake. Interestingly, our
578 results show that in other types of lakes, environmental variability leading to diatom thresholds may imply
579 different factors, as for instance climate-driven shifts in lake level beyond certain limits that may deeply
580 affect salinity conditions and ecosystem structure and functioning. In our case diatom threshold responses
581 seem to be coupled with climate thresholds (Maslin et al. 2013) caused by the abrupt climate events that
582 took place during the studied period. A higher resolution approach and additional case studies would
583 improve understanding of the magnitude and rate of change of the abrupt climate changes occurring during
584 this time period in the region, as well as the explicit detection of the character of ecological thresholds,
585 which cannot be properly identified at the resolution of the present study.

586 Pollen data show a landscape dominated by Steppe herbs and a fluctuating level of arboreal cover including
587 evidence of refuge areas, coherent with regional Late Glacial vegetation (González-Sampériz et al., 2004,

588 2005, 2010). Vegetation responded during cool-cold and arid periods (Late Glacial and Mystery Interval)
589 with the expansion of Steppe taxa while conifers (both *Juniperus* and *Pinus*) are the main arboreal
590 component, and Mesophytes and *Quercus* evolution must be associated to regional refuge areas. This
591 situation and the current resolution of this work does not enable the detection of potential abrupt responses
592 of vegetation to the environmental changes occurred during this time.

593

594 **5.7. Regional contextualization of the diatom record**

595 Reconstructions of the late Glacial and Early Holocene in the Mediterranean Basin using diatom data are
596 scarce. The Estanya diatom record is one of the first in the Iberian Peninsula to include that time periods. It
597 is in general agreement with other circum-Mediterranean records, which show a chronologically similar
598 pattern of climate change to north-western Europe and are characterised by alternations between cool,-arid
599 and warm-wet phases (see Wilson et al 2008 and literature therein). In the few regional records available for
600 the Late Glacial-Early Holocene period, diatom responses seem to be driven by both changing lake levels
601 and productivity, or a combination of the two. In L. Ioannina (Greece) facultative fragilaroid taxa indicative
602 of shallow water characterised Last Glaciation and Late Glacial periods indicating environmental and
603 physical stress, at times interrupted by peaks of *C. ocellata* and of benthic, eutrophic taxa associated with
604 episodes of lake deepening and rising productivity. The relative increase of planktonic taxa during the early
605 Late Glacial interstadial (14.5-14 cal kyr BP) reflected rising lake levels, which was followed by a decline
606 indicative of aridification during the Younger Dryas. During the Early Holocene a recovery of *C. ocellata*
607 suggested a lake deepening (Jones et al. 2013). In Lake Ohrid (Macedonia/Albania) *Cyclotella fotii*, a
608 species commonly found during former glacial phases, and *C. ocellata* prevailed during Late Glacial. The
609 apparent weak response of these diatoms to Late Glacial warming from 14.7 cal kyr BP to the Holocene
610 transition at 11.7 cal kyr BP was attributed to poor preservation but still needs confirmation (Reed et al.
611 2010). Diatom stratigraphy of Lago di Monticchio (southern Italy) is broadly described but shows that
612 during the Last Glaciation and Late Glacial Interstadial planktonic *Cyclotella comensis*, fragilaroid taxa and
613 other benthic diatoms dominated, indicating alkaline and oligotrophic to mesotrophic conditions. The
614 disappearance of *C.comensis* during the Younger Dryas event was attributed to lowered nutrient
615 concentrations in spite of increases in benthic fragilaroid taxa. From the Early Holocene, Laghi di

616 Monticchio evolved towards the modern-day fen that it is today, as reflected by diatoms characteristic of
617 very shallow lakes or marshes like *Cocconeis placentula* and *Nitzschia amphibia* (Watts et al. 1996). In
618 Lake Albano (central Italy), *Cyclotella* sp.1 prevailed until the Pleistocene/Holocene boundary, then
619 completely disappeared from the record, suggesting lake conditions quite unlike those occurring during the
620 majority of the Last Glaciation and Late Glacial that prevented the return of this species. It was replaced by
621 significant but fluctuating proportions of *Stephanodiscus hantzschii*, *C. ocellata* and fragilaroid taxa,
622 interpreted as responses to warming and changes in lake level and productivity. The Early Holocene was
623 dominated by small *Stephanodiscus* taxa reflecting a much a more productive lake (Ryves et al. 1996).
624 Similarly to these regional trends, in L. Estanya diatoms responded to climate-driven lake-level changes,
625 salinity fluctuations and habitat structure with assemblage replacements and sharp oscillation of diatom
626 accumulation rates. The absence in L. Estanya of diatom species demanding eutrophic conditions and the
627 prevalence of oligo-mesotrophic species suggest that fluctuations in lake productivity, as reflected in minor
628 shifts in diatom accumulation rates of *C. ocellata*, were driven more by climate related factors (epilimnetic
629 temperatures, evaporation, solar irradiation, etc) than by nutrient availability. Fragilaroid taxa,
630 characteristic of late glacial sediments in Mediterranean lakes and also in lakes of northern and central
631 Europe (Bradshaw et al. 2000, Lotter 2001, Birks et al. 2012) appeared in L. Estanya only in the context of
632 the cool and dry Late Glacial-Holocene boundary.

633

634 6. CONCLUSIONS

- 635 ▪ Lake Estanya contains an exceptional palaeoenvironmental and paleolimnological archive for the
636 last 20 cal kyr in continental Iberia.
- 637 ▪ As shown in other available circum-Mediterranean records, diatoms responded quickly to climate-
638 driven lake -level and salinity fluctuations associated to the humid/dry shifts during the last
639 glacial/interglacial transition. These climate changes triggered diatom responses particularly when
640 ecological threshold were crossed, especially during the stadial/interstadial episodes. The species-
641 specific responses observed suggest that the B/A interstadial could serve as a past analogue for
642 limnological responses with regard to current climate change.

- 643 ▪ Vegetation response during cool and arid periods (Late Glacial and Mystery Interval) was
644 characterized by an expansion of Steppe taxa. During the warmer and more humid phases of the
645 B/A interstadial, both Marcescent and Evergreen *Quercus* and aquatic vegetation expanded
646 following the general climate improvement. Increased presence of *Betula*, *Corylus* and *Quercus*
647 during cold periods such as the “Mystery interval” and the Younger Dryas suggest the presence of
648 local refuge areas for mesophytes during the Lateglacial.
- 649 ▪ Both diatom and regional vegetation show that wetter conditions typical of the Holocene onset were
650 delayed till 9.5 cal kyr BP, in agreement other continental sequences of the Iberian Peninsula. The
651 higher sensitivity of diatoms compared to vegetation to local abrupt climate changes during this
652 period suggest that in these mid altitude Mediterranean mountain settings the climate signal was
653 more rapidly transfer to the local limnological and hydrological subsystems than to the regional
654 vegetation.

655

656 **7. ACKNOWLEDGEMENTS**

657 This research has been funded through the projects LIMNOCLIBER (REN2003-09130-C02-02),
658 IBERLIMNO (CGL2005-20236-E/ CLI), LIMNOCAL (CGL2006-13327-C04-01), PALEODIVERSITAS
659 (CGL2006-02956/BOS), GLOBALKARST (CGL2009-08415), GRACCIE-CONSOLIDER (CSD2007-
660 00067), DINAMO (CGL2009-07992), DINAMO2 (CGL2012-33063); provided by the Spanish Inter-
661 Ministry Commission of Science and Technology. (CICYT); and PIRINEOSABRUPT (PM073/2007),
662 provided by the Diputación General de Aragón. Mario Morellón Marteles and Graciela Gil-Romera hold
663 post-doctoral contracts funded by the “JAE-Doc/CSIC” ref.- and “Juan de la Cierva” (grant ref. JCI2009)
664 programs respectively. Ana Pérez-Sanz has been supported by a PhD Fellowship provided by the Aragon
665 Government. We also thank Beatriz Bueno and Aída Adsuar for lab assistance. Finally, we are grateful to
666 Antonia Andrade Olalla for helping in initial pollen analyses and to Joan Gomà for assistance in diatom
667 taxonomic determinations. Two referee’s constructive criticism and suggestions helped improved a former
668 version of this paper.

669

670 **8. REFERENCES**

671 Abrantes, F., Gil, I., Lopes, C., Castro, M., 2005. Quantitative diatom analyses: a faster cleaning procedure.
672 Deep Sea Research 52:189–198.

673 Adrian, R., O'Reilly, C.M., Zagarese, H., Baines, B. S., Hessen, D.O., Keller, W., Livingstone, D. M.,
674 Sommaruga, R., Straile, D., Van Donk, E., Weyhenmeyer, G.A., Winder, M., 2009. Lakes as sentinels of
675 climate change. *Limnol Oceanography* 54(6): 2283-2297.

676 Ávila, A., Burrel, J.L., Domingo, A., Fernández, E., Godall, J., Llopart, J.M., 1984. Limnología del Lago
677 Grande de Estanya (Huesca). *Oecologia aquatica* 7, 3–24.

678 Battarbee, R.W., 1986. Diatom analysis. In: Berglund BE (ed.) *Handbook of holocene palaeoecology and*
679 *palaeohydrology*. Wiley, Chichester, pp 527–570.

680 Battarbee, R.W., Jones, V., Flower, R.J., Cameron, N.G., Bennion, H., Carvalho, L., Juggins, S., 2001.
681 Diatoms. In: Smol, J.P., Birks, H.J.B., Last, W.M. (eds.). *Tracking environmental change using lake*
682 *sediments*. Kluwer, Dordrecht.

683 Bennet, K.D., 1996. Determination of the number of zones in a biostratigraphical sequence. *New*
684 *Phytologist* 132: 155-170.

685 Bradshaw, E.G., Jones, V.J., Birks, H.B.J., Birks, H.H., 2000. Diatom responses to late-glacial and Early-
686 Holocene environmental changes at Kråkenes, western Norway. *Journal of Paleolimnology* 23: 21-34.

687 Birks, H.H., Jones, V.J., Brooks, S.J., Birks, H.J.B., Telford, R.J., Juggins, S., Peglar, S.M., 2012. From
688 cold to cool in northernmost Norway: Lateglacial and Early Holocene multi-proxy environmental and
689 climate reconstructions from Jansvatnet, Hammerfest. *Quaternary Science Reviews* 33, 100-120.

690 Blanco-Castro, E., Casado, M., Costa, M., Escribano, R., García Antón, M., Génova, M.,
691 Gómez, A., Moreno, J., Morla, C., Regato, P., Sainz Ollero, H., 1997. Los bosques ibéricos. Una
692 interpretación geobotánica. Planeta, Barcelona (Spain), 572 pp.

693 Bond, G., Heinrich, H., Broecker, W., Labeyrie, L., McManus, J., Huon, S., Tantschie, R., Clasen, S.,
694 Simet, C., Tedesco, K., Klas, M., Bonam, G., Ivy, S., 1992. Evidence for massive discharges into the North
695 Atlantic Ocean during the last glacial period. *Nature* 360, 245-249.

696 Broecker, W.S., 2000. Abrupt climate change: causal constraints provided by the palaeoclimate record.
697 *Earth-Science Reviews* 51, 137-154.

698 Broecker, W.S, 1994. Massive iceberg discharges as triggers for global climate change. *Nature* 372, 421-
699 424.

700 Cacho, I., Grimalt, J.O., Pelejero, C., Canals, M., Sierro, F.J., Flores, J.A., Shackleton, N., 1999.
701 Dansgaard- Oeschger and Heinrich event imprints in Alboran Sea paleotemperatures. *Paleoceanography* 14,
702 698-705.

703 Cacho, I., Grimalt, J.O., Canals, M., Sbaiffi, L., Shackleton, N.J., Schönfeld, J., Zahn, R., 2001.
704 Variability of the western Mediterranean Sea surface temperature during the last 25,000 years and its
705 connection with the Northern Hemisphere climatic changes. *Paleoceanography* 16, 40-52.

706 Cambra, J., 1991. Contribució a l'estudi de les algues epifítiques dels estanys de Banyoles, Basturs i
707 Estanya. *Orsis* 6, 27-44.

708 Carrión, J.S., 2002. Patterns and processes of Late Quaternary environmental change in a montane region of
709 southwestern Europe. *Quaternary Science Reviews* 21, 2047–2066.

710 Carrión, J.S., Fernández, S., González-Sampériz, P., Gil-Romera, G., Badald, E., Carrión-Marcod, Y,
711 López-Merino, L., López-Sáez, J.A., Fierro, E., Burjachs, F., 2010. Expected trends and surprises in the
712 Late Glacial and Holocene vegetation history of the Iberian Peninsula and Balearic Islands. *Review of*
713 *Palaeobotany and Palynology*, 162:458–475.

714 Cooper, S.R., 1995. Chesapeake Bay watershed historical land use: impact on water quality and diatom
715 communities. *Ecological Applications* 5,703–723.

716 Corella, J.P., El Amrani A., Sigró J., Morellón M., Rico E., Valero-Garcés, B., 2011. Recent evolution of
717 Lake Arreo, northern Spain: influences of land use change and climate. *J. Paleolimnology* 46, 469–
718 485.

719 Dansgaard, W., White, J.W.C., Johnsen, S.J., 1989. The abrupt termination of the Younger Dryas. *Nature*
720 339, 532-534.

721 Dansgaard, W., Johnsen, S. J., Clausen, H. B., Dahl-Jensen, D., Gundestrup, N. S., Hammer, C. U.,
722 Hvidberg, C. S., Steffensen, J. P., Sveinbjörnsdottir, A. E., Jouzel J., Bond, G., 1993. Evidence for general
723 instability of past climate from a 250-kyr ice-core record. *Nature* 364, 218 – 220.

724 Denton, G.H., Broecker, W., Alley, R.B., 2006. The Mystery Interval 17.5 to 14.5 kyr ago. In: Brigham-
725 Grette, J., Kull, C., Kiefer, T. (Eds.), *PAGES News* 14-16.

726 Denton, G.H., Anderson, R. F., Toggweiler, J. R., Edwards, R.L., Schaefer, J. M., Putnam, A. E., 2010.
727 The Last Glacial Termination. *Science* 328, 1652.

728 Dupré, M., 1992. *Palinología*. Sociedad Española de Geomorfología, 30 pp.

729 Fletcher, W.J., Sánchez Goñi, M.F., 2008. Orbital- and sub-orbital-scale climate impacts on vegetation of
730 the western Mediterranean basin over the last 48,000 yr. *Quaternary Research* 70, 451-464.

731 Flower, R.J., 1993. Diatom preservation: experiments and observations on dissolution and breakage in
732 modern and fossil material. *Hydrobiologia* 269/270, 473–484.

733 González-Sampériz, P., Valero-Garcés, B.L., Carrión, J.S., 2004. Was the Ebro valley a glacial refugium
734 for temperate trees? *Anales de Biología* 26: 13-20.

735 González-Sampériz, P., Valero-Garcés, B.L., Carrión, J.S., Peña-Monné, J.L., García-Ruiz, J.M., Martí-
736 Bono, C., 2005. Glacial and Lateglacial vegetation in northeastern Spain: New data and a review.
737 *Quaternary International* 140–141: 4–20.

738 González-Sampériz, P., Valero-Garcés, B.L., Moreno, A., Jalut, G., García-Ruiz, J.M.,
739 Martín-Bono, C., Delgado-Huertas, A., Navas, A., Otto, T., Dedoubat, J.J., 2006. Climate variability in the
740 Spanish Pyrenees during the last 30,000 yr revealed by the El Portalet sequence. *Quaternary Research* 66,
741 38–52.

742 González-Sampériz, P., Leroy, S.A.G., Fernández, S., García-Antón, M., Gil-García, M.J., Uzquiano, P.,
743 Valero-Garcés, B., Figueiral, I., 2010. Steppes, savannahs, forests and phytodiversity reservoirs during the
744 Pleistocene in the Iberian Peninsula. *Review of Palaeobotany and Palynology*, 162, 427-457

745 Grootes, P. M., Stuiver, M., White, James, W.C.J., Sigfus. J., Jouzel, J., 1993. Comparison of oxygen
746 isotope records from the GISP2 and GRIP Greenland ice cores. *Nature*, 366, 552-554.

747 Hammer, Ø., Harper, D.A.T., Ryan, P.D., 2001. PAST: Paleontological statistics software package for
748 education and data analysis. *Palaeontologia Electronica* 4(1), 9pp.

749 http://palaeoelectronica.org/2001_1/past/issue1_01.htm

750 Heegaard, E., Birks, H.J.B., Telford, R.J., 2005. Relationships between calibrated ages and depth in
751 stratigraphical sequences: an estimation procedure by mixed effect regression. *The Holocene*, 612–618.

752 Höbig, N., Weber, M.E., Kehl, M., Weniger, G.C., Julià, R., Melles, M., Fülöp, R.H., Vogel, H., Reicherter,
753 K., 2012. Lake Banyoles (northeastern Spain): A Last Glacial to Holocene multi-proxy study with regard to
754 environmental variability and human occupation. *Quaternary International* 274, 205-218.

755 Hofmann, G., M.Werum, H. Lange-Bertalot, 2011. *Diatomeen im Süßwasser-Benthos von Mitteleuropa*.
756 A.R.G. Gantner Verlag K.G.

757 IGME, 1982. *Mapa Geológico de España 1:50000 No. 289*. Benabarre. Instituto Geológico y Minero de
758 España, Madrid.

759 Huntley, B., Birks, H., 1983. *An atlas of past and present pollen maps for Europe: 0-13.000 years ago*.
760 Cambridge: Cambridge University Press. 667pp.

761 Jackson, S.T., Overpeck, J.T., 2000. Responses of plant populations and communities to
762 environmental changes of the late Quaternary. *Palaeobiology* 26 (Suppl.), 194-220.

763 Jalut, G., Marti, J.M., Fontugne, M., Delibrias, G., Vilaplana, J.M., Julia, R., 1992. Glacial to interglacial
764 vegetation changes in the northern and southern Pyrenees: deglaciation, vegetation cover and chronology.
765 *Quaternary Science Reviews* 11, 449–480.

766 Jones, T.D., Lawson, I.T., Reed, J.M., Wilson, G.P., Leng, M.J., Gierg, M., Bernasconi, S.M., Rienk, H.
767 Smittenberg, R.H., Hajdas, I., Bryant, Ch. L., Tzedakis, P.B., 2013. Diatom-inferred late Pleistocene and
768 Holocene palaeolimnological changes in the Ioannina basin, northwest Greece. *Journal of Paleolimnology*
769 49,185–204.

770 Krammer, K., 2002. *Diatoms of Europe. Diatoms of the European Inland Waters and Comparable Habitats*.
771 A.R.G.n Gantner Verlag K.G, Ruggell, p 584.

772 Krammer, K. , Lange-Bertalot, H., 1986. *Süßwasserflora von Mitteleuropa. Band 2*.
773 *Bacillariophyceae. Teil 1. Naviculaceae*. Gustav Fischer Verlag, Stuttgart.

774 Krammer, K. ,Lange-Bertalot, H., 1988. *Süßwasserflora von Mitteleuropa. Band 2*.
775 *Bacillariophyceae. Teil 2. Bacillariaceae, Epithemiaceae, Surirellaceae*. Gustav
776 Fischer Verlag, Stuttgart.

777 Krammer, K. and Lange-Bertalot, H., 1991. *Süßwasserflora von Mitteleuropa. Band 2*.
778 *Bacillariophyceae. Teil 3. Centrales, Fragilariaceae, Eunotiaceae*. Gustav
779 Fischer Verlag, Stuttgart.

780 Krammer, K. and Lange-Bertalot, H., 2001. Süßwasserflora von Mitteleuropa. Band 2.
781 Bacillariophyceae. Teil 4. Achnanthaceae, Kritische Ergänzungen zu Navicula
782 (Lineolatae) and Gomphonema [new edition]. Gustav Fischer Verlag, Stuttgart.
783 Lange-Bertalot, H., 2001a. Diatoms of the Europe inland waters and comparable habitats. A.R.G. Gantner
784 Verlag K.G., Ruggell, p 526.
785 Lange-Bertalot-Festschrift: Studies on Diatoms 2001b. Regine Jahn, John P. Kociolek, Andrzej Witkowski
786 & Pierre Compère Gantner (Eds.), Ruggell.
787 Last, W.M., Vance, R.E., 1997. Bedding characteristics of Holocene sediments from salt lakes of the
788 northern Great Plains, Western Canada. *Journal of Paleolimnology* 17, 297–318.
789 Lawson, I., Frogley, M., Bryant, C., Preece, R., Tzedakis, P., 2004. The Late Glacial and Holocene
790 environmental history of the Ioannina basin, north-west Greece, *Quaternary Science Review* 23, 1599–
791 1625.
792 Leira, M., 2005. Diatom responses to Holocene environmental changes in a small lake in northwest Spain.
793 *Quaternary International* 140/141, 90–102.
794 Leira, M., Santos, L., 2002. An Early Holocene short climatic event in the northwest Iberian Peninsula
795 inferred from pollen and diatoms. *Quaternary International* 93/94, 3–12.
796 Legendre, P., Legendre, L., 1998. *Numerical Ecology*, 2nd ed. Elsevier.
797 León-Llamazares, A., 1991. Caracterización agroclimática de la provincia de Huesca Ministerio de
798 Agricultura. Pesca y Alimentación (M.A.P.A.), Madrid.
799 Lotter, A.F., 2001. The paleolimnology of Soppensee (central Switzerland), as evidenced by diatom, pollen,
800 and fossil pigments analyses. *Journal of Paleolimnology* 25, 65-79.
801 López-Vicente, M., 2007. Erosión y redistribución del suelo en agroecosistemas mediterráneos:
802 Modelización predictiva mediante SIG y validación con ¹³⁷Cs (Cuenca de Estaña, Pirineo Central). PhD
803 Thesis, Universidad de Zaragoza. Zaragoza, 212 pp.
804 Montserrat J., 1992. Evolución glacial y postglacial del clima y la vegetación en la vertiente sur del Pirineo:
805 Estudio palinológico. Instituto Pirenaico de Ecología-CSIC, Zaragoza.
806 Moore P.D. & Webb J.A. ,1978. *An Illustrated Guide to Pollen Analysis*. Wiley and Sons.

807 Morellón, M., Valero-Garcés, B.L., Anselmetti, F., Ariztegui, D., Schnellmann, M., Moreno, A., Mata, P.,
808 Rico, M., Corella, J.P., 2009a. Late Quaternary deposition and facies model for karstic Lake Estanya (NE
809 Spain). *Sedimentology*, 1505-1534.

810 Morellón M., Valero-Garcés B., Vegas-Vilarrúbia T, González-Sampéris P., Romero O., Delgado-Huertas
811 A., Mata P., Moreno A., Rico M., Corella JP., 2009b. Late Glacial and Holocene palaeohydrology in the
812 western Mediterranean region: The Lake Estanya record (NE Spain). *Quaternary Science Reviews* 28,
813 2582–2599.

814 Moreno, A., Cacho, I., Canals, M., Prins, M.A., Sánchez-Goñi, M.F., Grimalt, J.O., Weltje, G.J., 2002.
815 Saharan dust transport and high latitude glacial climatic variability: the Alboran Sea record. *Quaternary*
816 *Research* 58, 318-328.

817 Moreno, A., Stoll H., Jiménez-Sánchez M., Cacho I., Valero-Garcés B., Emi Ito, Edwards L.E.R., 2010.
818 A speleothem record of glacial (25–11.6 kyr BP) rapid climatic changes from northern Iberian Peninsula.
819 *Global and Planetary Change* 71, 218–231.

820 Moreno, A., López-Merino, L., Leira, M., Marco-Barba, J., González-Sampéris, P., Valero-Garcés, B.,
821 López-Sáez, J.A., Santos, L., Mata, P., Ito, E., 2011. Revealing the last 13,500 years of environmental
822 history from the multiproxy record of a mountain lake (Lago Enol, northern Iberian Peninsula). *Journal of*
823 *Paleolimnology* 46, 327-349.

824 Moreno, A., González-Sampéris, P., Mario Morellón, M., Valero-Garcés, B., Fletcher W.J., 2012. Northern
825 Iberian abrupt climate change dynamics during the last glacial cycle: A view from lacustrine sediments.
826 *Quaternary Science Review* 36, 139-153.

827 Pérez-Bielsa, C., Lambán, L., Plata, J., Rubio, F., Soto, R., 2012. Characterization of a karstic aquifer using
828 magnetic resonance sounding and electrical resistivity tomography: a case-study of Estaña Lakes (northern
829 Spain). *Hydrogeology Journal* 20, 1045-1059.

830 Pérez-Obiol, R., Julià, R., 1994. Climatic change on the Iberian Peninsula recorded in a 30,000-yr pollen
831 record from Lake Banyoles. *Quaternary Research* 41, 91-98.

832 Pérez-Sanz, A., González-Sampéris, P., Moreno, A., Valero-Garcés, B., Gil-Romera, G., Rieradevall, M.,
833 Tarrats, P., Lasheras-Álvarez, L., Morellón, M., Belmonte, A., Sancho, C., Sevilla-Callejo, M., Navas A.,

834 2013. Holocene climate variability, vegetation dynamics and fire regimen in the Central Pyrenees: the Basa
835 de la Mora sequence (NE Spain). *Quaternary Sciences Review* 73, 149-169.

836 Poulíčková, A., Hašler, P., 2007. Aerophytic diatoms from caves in central Moravia (Czech Republic).
837 *Preslia* 79, 185–204.

838 Reed, J. M., 1998. A diatom conductivity transfer function for Spanish salt lakes. *Journal of Paleolimnology*
839 19, 399–416.

840 Reed, J.M., Stevenson, A.C., Juggins, S., 2001. A multi-proxy record of Holocene climatic change in
841 southwestern Spain: the Laguna de Medina, Cadiz. *The Holocene* 11, 707-719.

842 Reed, J.M., Cvetkoska, A., Levkov, Z., Vogel, H., Wagner, B., 2010. The last glacial-interglacial cycle in
843 Lake Ohrid (Macedonia/ Albania): testing diatom response to climate. *Biogeosciences* 7, 3083–3094.

844 Reille, M., Lowe, J.L., 1993. A re-evaluation of the vegetation history of the eastern Pyrenees (France)
845 from the end of the last glacial to the present. *Quaternary Science Reviews* 12, 47–77.

846 Reimer, P.J., Baillie, M.G.L., Bard, E., Bayliss, A., Beck, J.W., Bertrand, C.J.H., Blackwell, P.G., Buck,
847 C.E., Burr, G.S., Cutler, K.B., Damon, P.E., Edwards, R.L., Fairbanks, R.G., Friedrich, M., Guilderson,
848 T.P., Hogg, A.G., Hughen, K.A., Kromer, B., McCormac, G., Manning, S., Ramsey, C.B., Reimer, R.W.,
849 Remmele, S., Southon, J.R., Stuiver, M., Talamo, S., Taylor, F.W., van der Plicht, J., Weyhenmeyer, C.E.,
850 2004. IntCal04 terrestrial radiocarbon age calibration, 0–26 cal kyr BP. *Radiocarbon* 46, 1029–1058.

851 Reimer, P.J., Baillie, M.G.L., Bard, E., Bayliss, A., Beck, J.W., Blackwell, P.G., Ramsey, C.B., Buck, C.E.,
852 Burr, G.S., Edwards, R.L., Friedrich, M., Grootes, P.M., Guilderson, T.P., Hajdas, I., Heaton, T.J., Hogg,
853 A.G., Hughen, K.A., Kaiser, K.F., Kromer, B., McCormac, F.G., Manning, S.W., Reimer, R.W., Richards,
854 D.A., Southon, J.R., Talamo, S., Turney, C.S.M., van der Plicht, J., Weyhenmeyer, C.E., 2011. IntCal09
855 and Marine09 Radiocarbon Age Calibration Curves, 0-50,000 Years cal BP.

856 Riera, S., Wansard, G., Julià, R., 2004. 2000-year environmental history of a karstic lake in the
857 Mediterranean Pre-Pyrenees: the Estanya lakes (Spain). *Catena* 55, 293–324

858 Ryves, D.B., Juggins, S., Fritz, S.C., Battarbee, R.W., 2001. Experimental diatom dissolution and the
859 quantification of microfossil preservation in sediments. *Palaeogeography, Palaeoclimatology,*
860 *Palaeoecology* 1172, 99–113.

861 Ryves, D.B., Jones, V.J., Guilizzoni, P., Lami, A., Marchetto, A., Battarbee, R.W., Bettinetti, R., Devoy,
862 E.C., 1996. Late Pleistocene and Holocene environmental changes in Lake Albano and Lake Nemi (central
863 Italy) as indicated by algal remains. *Memorie dell' Istituto Italiano di Idrobiologia*. 55: 119- 148.

864 Taylor, K.C., Mayewski, P. A., Alley, R. B., Brook, E. J., Gow, A. J., Grootes, P. M., Meese, D. A.,
865 Saltzman, E. S., Severinghaus, J. P., Twickler, M. S., White, J. W. C, Whitlow, S., Zielinski, G. A.,
866 1997. The Holocene-Younger Dryas Transition Recorded at Summit, Greenland. *Science* 278, 5-827.

867 Steffensen, J.P., Andersen, K.K., Bigler, M., Claussen, H.B., Dahl-Jensen, D., Fischer, H.,
868 Goto-Azuma, K., Hanson, M., Johnsen, S.J., Jouzel, J., Masson-Delmotte, V., Popp, T., Rasmussen, S.O.,
869 Röthlisberger, R., Ruth, U., Stauffer, B., Siggaard-Andersen, M.L., Sveinbjörnsdóttir, A.E.,
870 Stockmarr J., 1973. Determination of spore concentration with an electronic particle counter. *Danmarks*
871 *geologiske Undersøgelse Årbog*, 1972, 87–89.

872 Svenson, A., White, J.W.C., 2008. High resolution Greenland ice core data show abrupt climate change
873 happens in few years. *Science* 321, 680-684.

874 ter Braak C. J. E, Verdonschot, Piet, E.M., 1995. Canonical correspondence analysis and related multivariate
875 methods in aquatic ecology. *Aquatic Sciences* 57/3, 255-289.

876 Valero-Garcés, B.L., Kelts, K.R., 1995. A sedimentary facies model for perennial and meromictic saline
877 lakes: Holocene Medicine Lake Basin, South Dakota, USA. *Journal of Paleolimnology* 14, 123–149.

878 Valero-Garcés, B., Zeroual, E., Kelts, K., 1998. Arid phase in the western Mediterranean region during the
879 last glacial cycle reconstructed from lacustrine records. In: Benito, G., Baker, V.R., Gregory, K.J. (Eds.),
880 *Paleohydrology and Environmental Change*. Wiley, London, pp. 67-80.

881 Valero-Garcés, B., Gonzalez-Samperiz, P., Delgado-Huertas, A., Navas, A., Machin, J., Kelts, K., 2000.
882 Lateglacial and Late Holocene environmental vegetational change in Salada Mediana, central Ebro Basin,
883 Spain. *Quaternary International* 73–74, 29–46.

884 Van Dam, H., Mertens, A., Sinkeldam, J., 1994. A coded checklist and ecological indicator values
885 of freshwater diatoms from the Netherlands. *Netherlands Journal of Aquatic Ecology* 28, 117-133.

886 Vegas-Vilarrúbia T., Rull V., Montoya E., Safont E., 2011. Quaternary palaeoecology and nature
887 conservation: a general review with examples from the neotropics. *Quaternary Science Reviews* 30, 2361-
888 2388.

889 Weninger, B., Jöris, O., 2004. Glacial radiocarbon calibration. The CalPal Program. In: Higham, T.,
890 Ramsey, C.B., Owen, C. (Eds.), Radiocarbon and Archaeology. Fourth International Symposium, Oxford
891 2002.
892 Witkowski, A., Lange-Bertalot, H., Metzeltin, D., 2000. Diatom flora of marine coasts. In: Lange-Bertalot
893 H (Ed.) Iconographia diatomologica, p 925.

894
895

896 **FIGURE CAPTIONS:**

897

898 Figure 1: (A) Topographic and geological map of ‘Balsas de Estanya’s catchment area. The location of the
899 study area is indicated with a star. (B) Bathymetry of the main lake, Estanque Grande de Abajo with coring
900 sites (1A to 5A).

901

902 Figure 2: Updated chronological model for the Lake Estanya sequence (A) and detail of the time interval
903 studied in this paper (19.7 to 9.3 cal kyr BP). The continuous line represents the age-depth function framed
904 by dashed lines (error lines). Sedimentary units and limits of cores used for the composite sequence are also
905 displayed at the right end.

906

907 Figure 3: A) Relative abundance ($\geq 3\%$) of diatom taxa throughout the record. The dotted lines separate
908 diatom zones DZ-EST-1 to DZ-EST-5. Valve accumulation rates in valves $\cdot \text{cm}^{-2} \cdot \text{year}^{-1}$. Radiocarbon
909 (^{14}C) dates in calibrated years before present (BP). B) Zone DZ-EST-2 is subdivided in eleven subzones (a-
910 k). Correlation between diatom abundance and the $\delta 18\text{O}$ GRIP Greenland ice-core showing main climatic
911 features on the new event chronology proposed by the INTIMATE group (Björk et al. 1998) and its
912 correspondence with the classic last deglaciation sequence of GISPS2 (Stuiver et al. 1995).

913

914 Figure 4: CCA ordination diagram representing XRF geochemical variables, site scores (depths)
915 and species scores across axes: 4a and 4b: axes 1 and 2; 4c and 4d, axes 2 and 3. A: *Cyclotella ocellata*, B:
916 *Cyclotella distinguenda*, C: *Amphora inariensis*, D: *Amphora lybica*, E: *Amphora veneta* var. *sub capitata*,

917 F: *Amphora* spp, G: *Brachysira vitrea*, H: *Cocconeis placentula*, I: *Cymbella* sp.1, J: *Denticula elegans*, K:
918 *Diploneis ovalis*, L: *Encyonopsis caespitosa*, M: *Encyonopsis microcephala*, N: *Encynopsis subminuta*, O:
919 *Ephitemia adnata*, P: *Fallacia cf pygmaea*, Q: *Hantzschia amphioxus*, R: *Hyppodonta hungarica*, S:
920 *Luticula mutica*, T: *Luticula nivalis*, U: *Mastogloia braunii*, V: *Mastogloia smithii*, WW: *Mastogloia* spp,
921 X: *Navicula salinarum*, Y: *Navicula subalpina*, Z: *Navicula* spp, AA: *Navicula* sp.2, BB: *Navicula* sp. 11,
922 CC: *Navicula* sp. 4, DD: *Navicula* sp. 9, EE: *Nitzschia cf. filiformis*, FF: *Nitzschia hungarica*, GG:
923 *Nitzschia incospicua*, HH: *Pinnularia borealis*, II: *Pinnularia* spp, JJ: *Pseudostaurosira brevistriata*, KK:
924 *Sellaphora pupula*.

925 Figure 5: Pollen diagram of selected taxa and group taxa from the Lateglacial to Holocene
926 transition of Estanya lake record. Other Mesophytes curve includes *Alnus*, *Carpinus*, *Salix*, *Ulmus*,
927 *Populus*, *Tilia*, *Fagus*, *Acer*, *Fraxinus* and *Juglans*. Mediterranean shrubs is composed of *Pistacia*,
928 *Rhamnus*, *Phyllyrea*, *Buxus* and *Sambucus*, and Steppe taxa by *Ephedra distachya*, *E. fragilis*,
929 *Artemisia*, Cichorioideae, Asteroideae, Carduae, Chenopodiaceae and *Plantago*.

930
931 Figure 6: Summary record grouping diatoms, according to their known habitat preferences, and main pollen
932 assemblages. Diatom and pollen records are correlated with paleohydrological, paleoenvironmental and
933 paleoclimatic records: sedimentary units and lake level reconstruction are based on sedimentary facies and
934 geochemically-based salinity estimations (Morellón 2009b), and finally the $\delta^{18}\text{O}$ GRIP Greenland ice-core
935 showing the new event chronology proposed by the IMITATE group 2 and its correspondence with the
936 classical last deglaciation sequence of GISPS2. Main climate events are delimited by the dotted lines and
937 white/grey bars.

938

939

940

941

942

943

944

945

946

947

Table 1[Click here to download Table: Table 1.doc](#)

Table 1: Eigenvalues and constraining percentages of main eigenvectors. Correlations between environmental variables and eigenvectors. Asterisks indicate significant correlations ($p = 0,1$, one-tailed probabilities).

	Axis 1	Axis 2	Axis 3
Eigenvalue	0.390	0.290	0.204
Percentage	34.7	25.4	18.2
Correlations			
Al	0.22	-0.12	-0.16
Si	-0.12	-0.02	-0.25
S	0.38*	0.25	0.11
K	-0.18	-0.12	-0.34*
Ca	0.47*	-0.22	0.26
Ti	-0.26	0.00	-0.31*
Fe	-0.44*	-0.06	-0.33*

Figure 1
[Click here to download high resolution image](#)

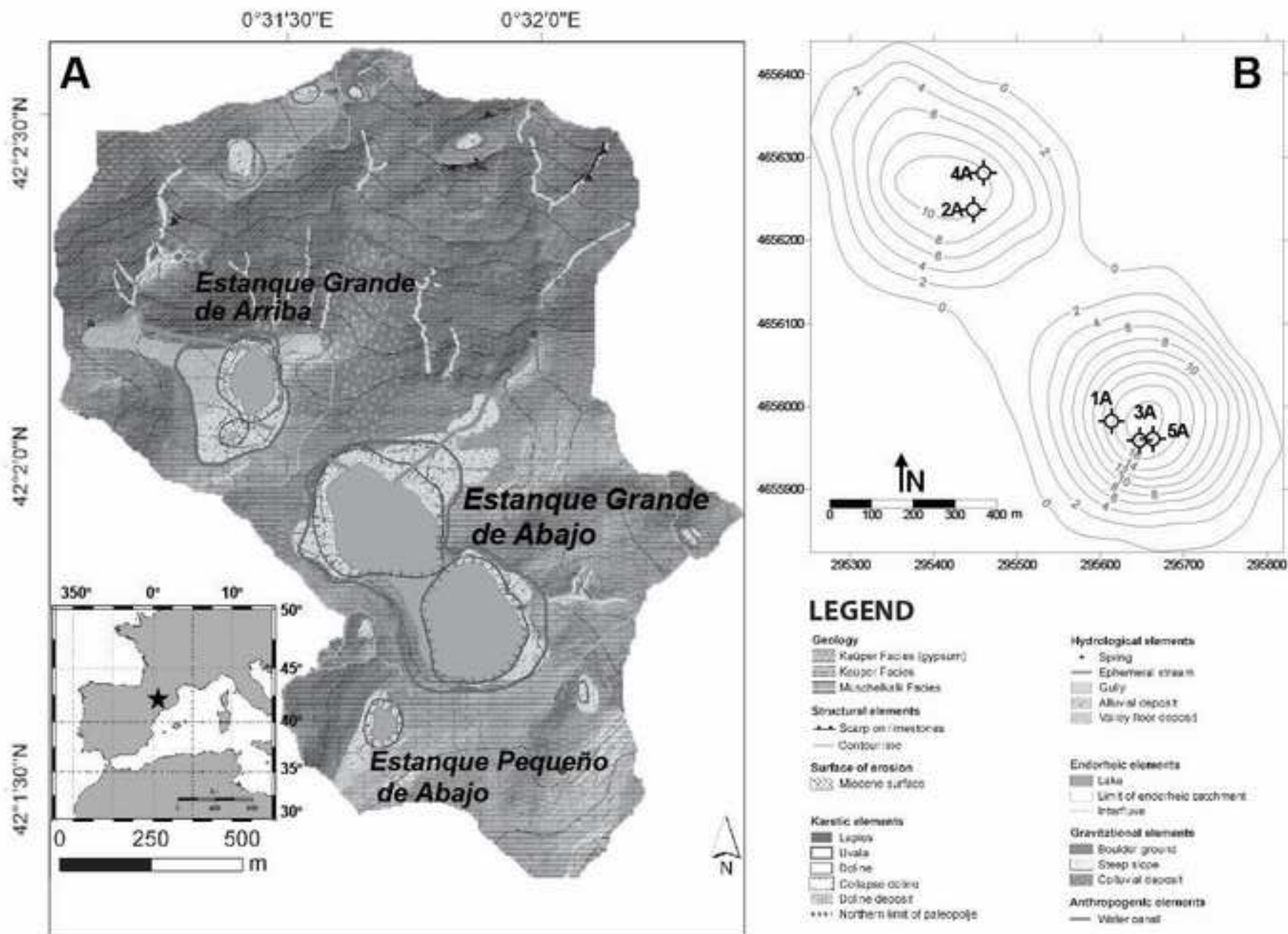


Figure 2
[Click here to download high resolution image](#)

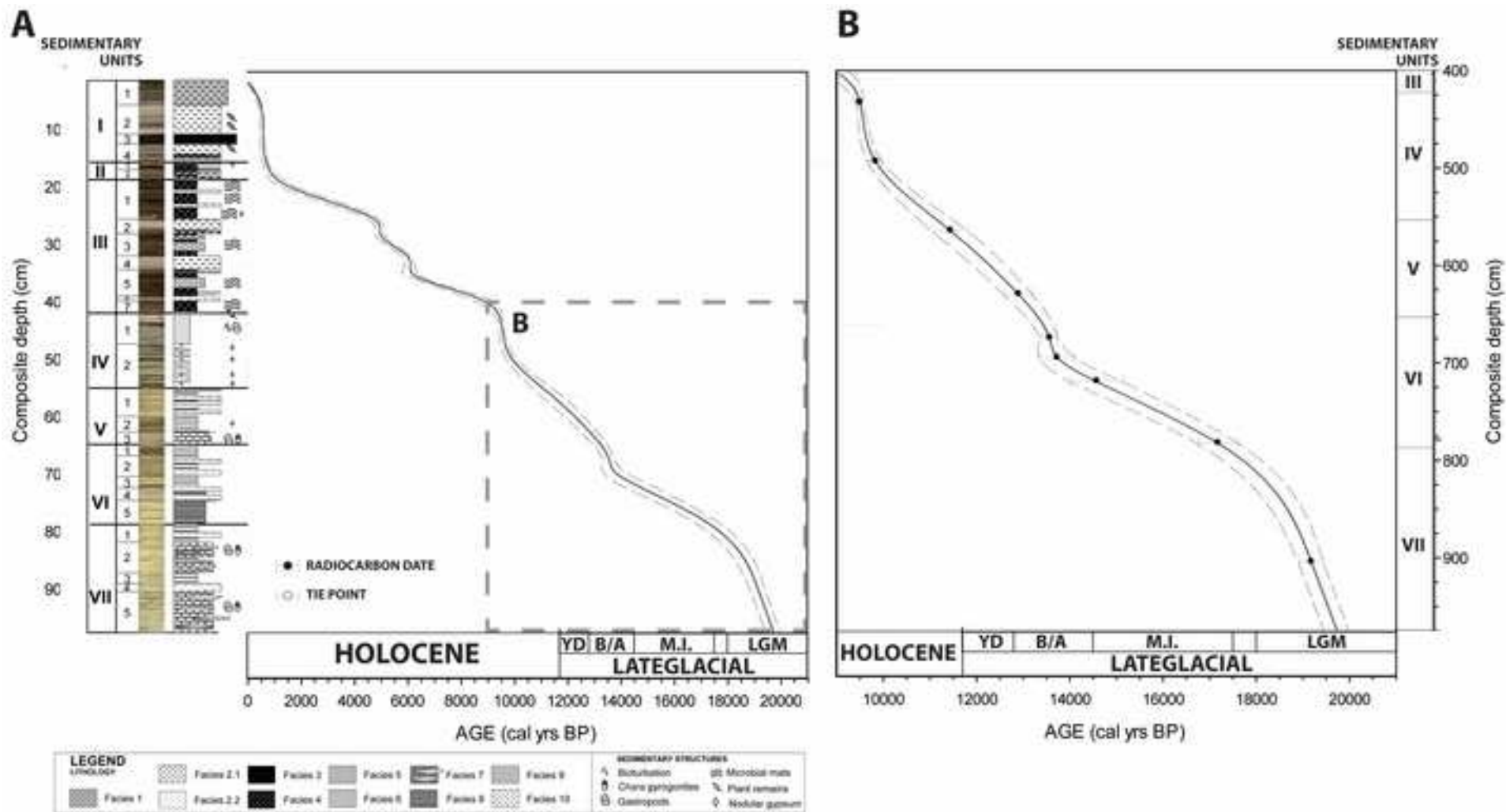


Figure 3
[Click here to download high resolution image](#)

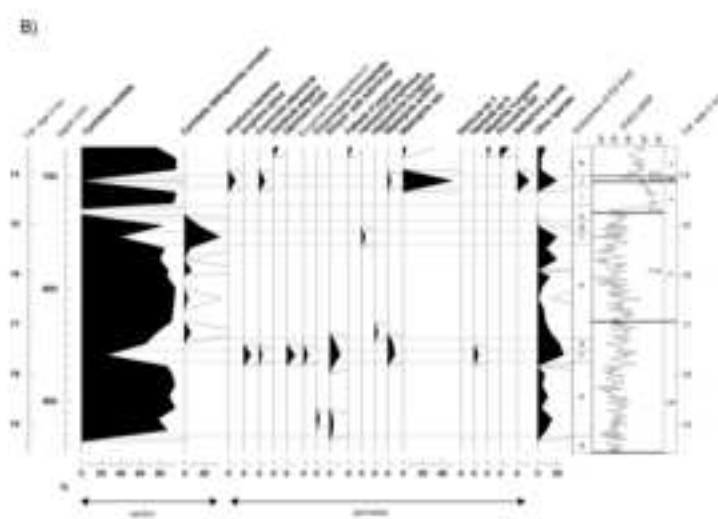
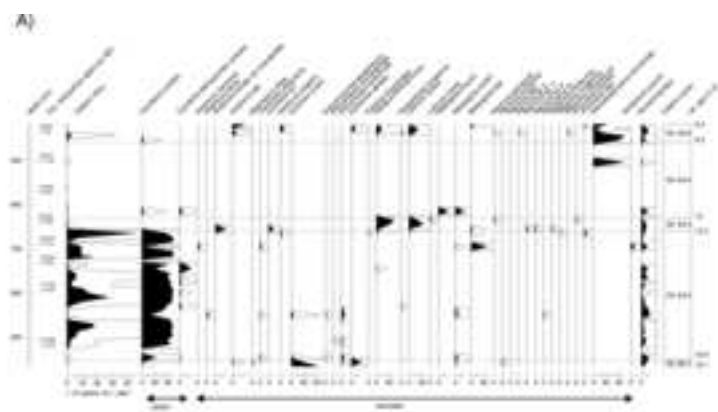


Figure 4
[Click here to download high resolution image](#)

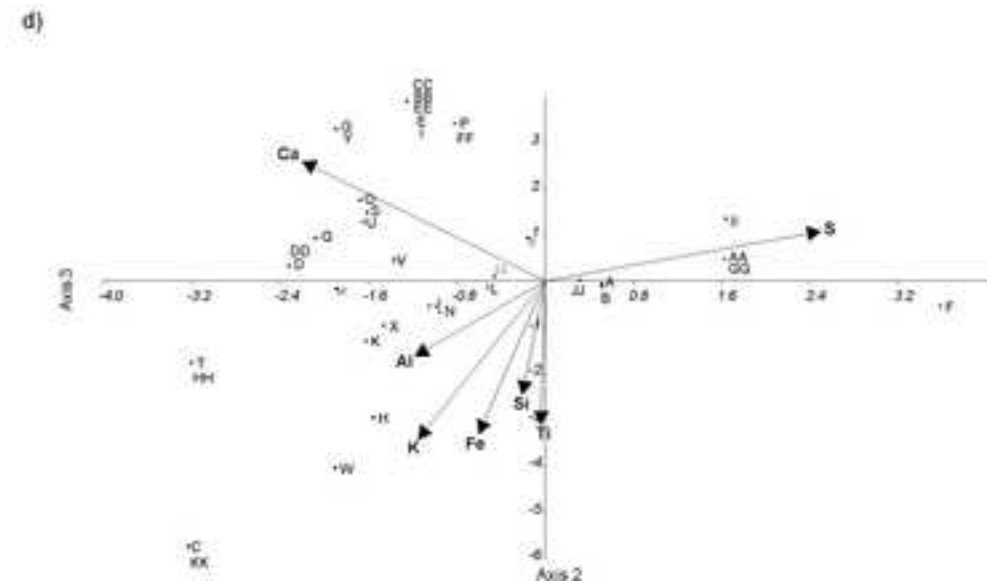
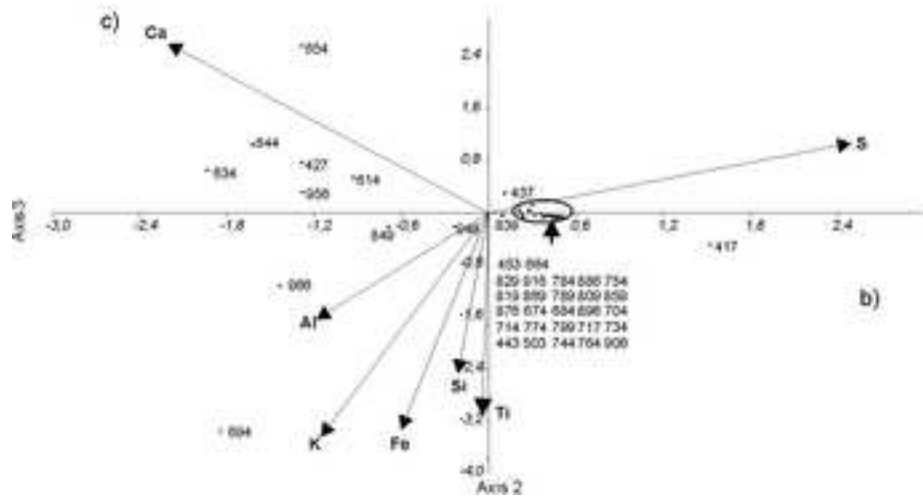
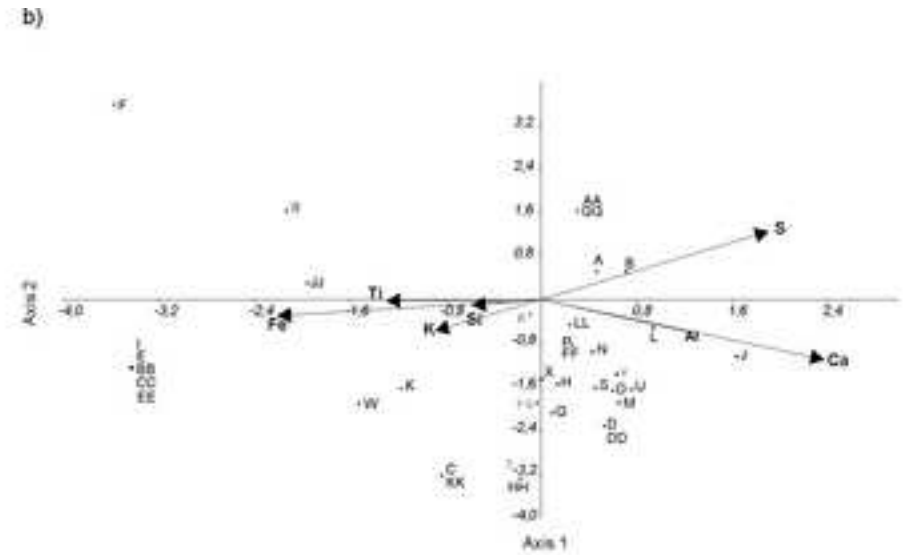
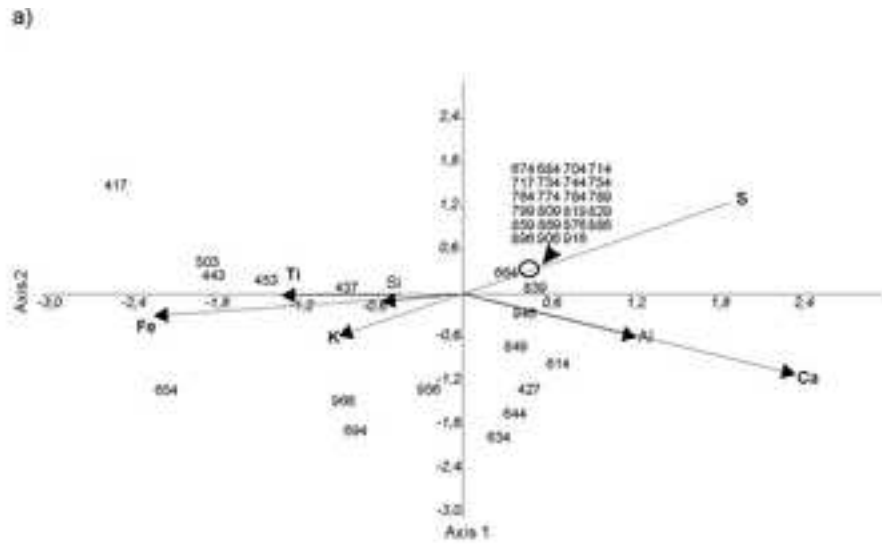


Figure 6
[Click here to download high resolution image](#)

